


RESEARCH

Open Access



Acute targeting of N-terminal tau protein has long-lasting beneficial effects in Tg2576 APP/A β mouse model by reducing cognitive impairment, cerebral A β -amyloidosis, synaptic remodeling and microgliosis later in life

Valentina Latina^{1,2}, Margherita De Intron^{3,4}, Francesca Malerba^{2,5}, Rita Florio², Bijorn Omar Balzamino⁶, Giuseppe Di Natale⁷, Michele Francesco Maria Sciacca⁷, Giuseppe Pappalardo⁷, Alessandra Micera⁶, Annabella Pignataro^{1,3}, Pietro Calissano^{2†} and Giuseppina Amadoro^{1,2*†} 

Abstract

Even though the number of patients suffering from Alzheimer's Disease (AD) is rapidly growing worldwide, only a few symptomatic treatments have been approved for clinical use, pointing out the urgent need for more effective disease-modifying therapies that actually alter the progression of this neurodegenerative disorder which is characterized by co-occurrence of both Amyloid beta (A β) and tau neuropathologies. Preclinical and clinical evidence suggests that a link between A β and tau drives the entire continuum of AD pathobiology. 12A12 is a monoclonal antibody (mAb) which offers neuroprotection into two transgenic lines of AD, including Tg2576 that overexpresses Swedish mutation (KM670/671NL) of Amyloid Precursor Protein (APP, isoform 695) and 3xTg (APP Swedish, MAPT P301L, and PSEN1 M146V), by targeting the 20–22kDa N-terminal tau fragments (NH₂htau). In particular, acute (over 14 days with 4 doses), intravenous injection of 12A12mAb leads to significant improvement of cognitive, biochemical and histopathological AD signs in symptomatic 6-month-old Tg2576, a well-established transgenic mouse model that mimics the human amyloidosis with an age-dependent A β accumulation/aggregation and plaque deposition. Here, we report that Tg2576 mice, immunized with 12A12mAb at 6 months of age and returned to their home cage for additional 3 months, exhibit preserved spatial memory despite the anticipated interruption of antibody administration (discontinuous treatment). This enduring beneficial effect on memory deficit (up to 90 days after the last injection) is accompanied by normalization in the synaptic imbalance and microgliosis along with decrease of the most toxic A11-positive prefibrillar oligomers and inverse increase in 4kDa monomeric form(s) of A β 1–42. These findings reveal that: (i) soluble, pathogenetic tau specie(s) located at the N-terminal domain of protein early synergizes with A β in driving the progression of AD neuropathology; (ii) transient immunoneutralization of the NH₂htau following short-term treatment with 12A12mAb exerts preventive, long-lasting neuroprotective effects, at least in part by interfering

[†]Pietro Calissano and Giuseppina Amadoro have equally shared the seniorship of the work.

*Correspondence:

Giuseppina Amadoro
g.amadoro@inmm.cnr.it

Full list of author information is available at the end of the article



© The Author(s) 2025. **Open Access** This article is licensed under a Creative Commons Attribution-NonCommercial-NoDerivatives 4.0 International License, which permits any non-commercial use, sharing, distribution and reproduction in any medium or format, as long as you give appropriate credit to the original author(s) and the source, provide a link to the Creative Commons licence, and indicate if you modified the licensed material. You do not have permission under this licence to share adapted material derived from this article or parts of it. The images or other third party material in this article are included in the article's Creative Commons licence, unless indicated otherwise in a credit line to the material. If material is not included in the article's Creative Commons licence and your intended use is not permitted by statutory regulation or exceeds the permitted use, you will need to obtain permission directly from the copyright holder. To view a copy of this licence, visit <http://creativecommons.org/licenses/by-nc-nd/4.0/>.

at “pre-plaque” stage with the progressive deposition of insoluble, fibrillar A β via a shift of its aggregation pathway into its less harmful, unaggregated monomeric forms. Taken together, these findings represent a strong rationale for the advancement of 12A12mAb to clinical stage aiming at preventing the A β -dependent neurodegeneration by lowering the cerebral levels of NH $_2$ tau in humans suffering from chronic, slow-progressing AD.

Keywords Alzheimer’s Disease (AD), Tau protein, Amyloid beta (A β), Preclinical animal model, Immunotherapy

Introduction

Lesson learnt from ongoing medical trials in humans has shown that combination immunotherapy against both the pathogenic A β and tau is likely to be more successful in counteracting the development of Alzheimer’s Disease (AD) [1–4], a complex neurodegenerative disorder that accounts for 60–80% of cases of dementia worldwide among the elderly people [5, 6]. Clinical and experimental evidence both in cellular and animal models have shown that A β and tau, directly and/or indirectly, interact with each other in the promotion of cognitive decline and that this reciprocal interplay is more likely to recapitulate the spatiotemporal progression of human AD continuum [7–14]. With this in mind, the implementation of current therapeutic regimens with two or more disease-modifying agents targeting both neuropathologies, given at smaller and potentially safer doses in concomitance or even in sequence across the biological evolution of disease, is desirable in order to have higher clinical benefit, tolerability and safety with consequent amelioration in compliance of affected patients [15]. However, it is still a matter of debate whether a linear cause-effect or a co-pathogenic interaction between A β and tau is required over time to drive the gradual clinical trajectory of AD manifestation [16–18].

More recently, we have shown that acute (i.e. 4 doses over 14 days), intravenous (i.v.) immunization with monoclonal antibody (mAb) 12 A12 is effective in mitigating the memory/learning deficits and related biochemical, morphological and functional deterioration in both 6-month-old Tg2576 (Swedish mutation KM670/671 NL of Amyloid Precursor Protein (APP)) and 3xTg (APP Swedish, MAPT P301L, and PSEN1 M146 V) mice by targeting the 20–22kDa N-terminal tau fragments (NH $_2$ tau) [1, 2, 19–23]. Even though current AD mouse models do not recapitulate all the full aspects of the human neuropathology, Tg2576 mice display a gradual A β accumulation/aggregation into their brains [24]. This makes them suitable for examining the temporal correlation between the rate of A β deposition and the extent of neuronal damage in the presence of an endogenous background of not-mutated tau, just as in AD [25]. In particular, the cumulative cerebral amyloidosis increases in detergent insoluble A β starting at ~6 months

of age followed by amyloid plaques deposition from 10–11 months up to 23 months [26] ending in classic neuritic plaques with Congo red-positive amyloid cores that are similar to those seen in AD subjects [27]. Despite the fact that they do not develop late neurofibrillary tangles (NFTs), starting from 3 months of age Tg2576 mice show the pattern of most toxic (hyperphosphorylated and cleaved and misfolded/oligomeric), soluble species proximal to the onset of tau pathology, just as other APP-overexpressing model [2, 28]. Relevantly, in this strain the treatment with 12 A12 mAb positively impacts not only on tau but also upstream on APP/A β neuropathology [2, 21, 22], further supporting the potential of N-terminal end of tau protein as valid target for disease-modifying therapy of AD [29–31].

Thus, to move forward the preclinical characterization of 12 A12 mAb toward clinical translation, we investigated how long the protective action of its short-term non-invasive administration is sustained in these APP-overexpressing mice after cessation of the last injection (discontinuous regimen). This was accomplished by assessing four classic, phenotype-associated read-outs including the recognition memory performance, the extent of both tau and A β pathology, synaptic protein expression and gliosis. To this aim, Tg2576 animals were immunized at the age of 6 months (i.e. when they are cognitively impaired with a moderate accumulation of pathogenic NH $_2$ tau into their hippocampi), aged for additional 3 months (“washout phase”) and, then, analyzed at more severe stage of disease (i.e. 9 months of age when A β seeds undergo deposition in concomitance with a high burden of hippocampal NH $_2$ tau but insoluble, fibrillar A β plaques are not still clearly detectable).

Materials and methods

Animals and ethical approval

All animal experiments were complied with the ARRIVE guidelines and were carried out in accordance with the ethical guidelines, the European Council Directive (2010/63/EU) and the Italian Animal Welfare legislation (D.L. 26/2014). The experimental approval was obtained from the Italian Ministry of Health (Authorization n. 1038–2020-PR; Authorization n. 419/2023-PR). This

study was carried out according to the principles of the 3Rs (Replacement, Reduction and Refinement) to minimize animal suffering and to reduce the number of animals used.

Heterozygous Tg2576 mice of both genders (Tg), expressing the human Amyloid Precursor Protein (APP) with the Swedish mutation KM670/671 NL [24] which causes an increase in A β production [32] and their wild-type (Wt) littermates were used at 6 months of age ($n = 8-10$ per group) in the immunization regimen. Genotyping was carried out to confirm the presence of human mutant APP DNA sequence by PCR.

Immunization scheme

The N-terminal tau 12 A12 antibody (26–36aa) –(formerly Caspase-Cleaved protein-NH₂4268 tau antiserum, [33]– was produced and characterized by monoclonal antibodies core facility at EMBL—Monterotondo, Rome, Italy (Dott. Alan Sawyer), as previously described in [34]. This cleavage site-directed monoclonal antibody (mAb) (i.e. for the detection of specific peptide bond cleavage) [35, 36] was generated by immunizing mice with a peptide of 26–36aa of hT40 (D₂₅(NH₂-QGGYTMHQDQ-COOH epitope), which encompasses a conserved caspase(s)-cleavage site previously identified in cellular and animal Alzheimer's disease models [37] and in human Alzheimer's disease brains [36]. 12 A12 mAb was produced and purified from hybridoma supernatants according to standard procedures, as previously described in [2] and its cleavage-site specificity was verified by enzyme-linked immunosorbent assay (ELISA) test (95% sensitivity and 90% specificity) by using the two overlapping sequences of htau 40:

Ac : QGGYTMHQDQEGDQTDAGLKC – amide; cleavage site peptide (1)

Ac : YGLGDRKDQGGYTMHQDQC – amide; spanning site peptide (2)

12 A12 was validated on the basis of its specific binding to the immunogen cleavage-sequence peptide (1)

and contextually for the absence of binding to the spanning peptide (2) used as negative control (Suppl.Fig. 1 A), as reported for antibodies that react preferentially with a cleavage product following the action of a proteolytic enzyme without altering the expression level of full-length protein [35, 38, 39].

6-month-old mice were randomized into: (1) wild-type mice treated with saline vehicle; (2) age-matched Tg2576 mice treated with saline vehicle; (3) age-matched Tg2576 mice treated with 12 A12 mAb (30 μ g/dose). Animals were acutely infused over 14 days with two weekly injections administered on two alternate days (4 doses) to the lateral vein of the tail. The dose and route of immunization and the efficacy of this 14 days treatment were based on previously published studies by our and other independent research groups using Tg2576 mice as APP/A β transgenic mouse model [2, 21–23]. After the last injection, animals were housed for additional three months. The housing conditions (four or five animals per cage) in pathogen-free facilities were controlled (temperature 22 °C, 12 h light/12 h dark cycles, humidity 50–60%) with ad libitum access to food and water. Animals were examined in their overall health, home cage nesting, sleeping, feeding, grooming, and condition of the fur and body weight throughout the whole study and any gross abnormalities were noted. 90 days after the last injection (discontinuous treatment), animals of 9 months of age underwent behavioural test or were sacrificed for biochemical and morphological analyses.

Antibody availability in the hippocampus

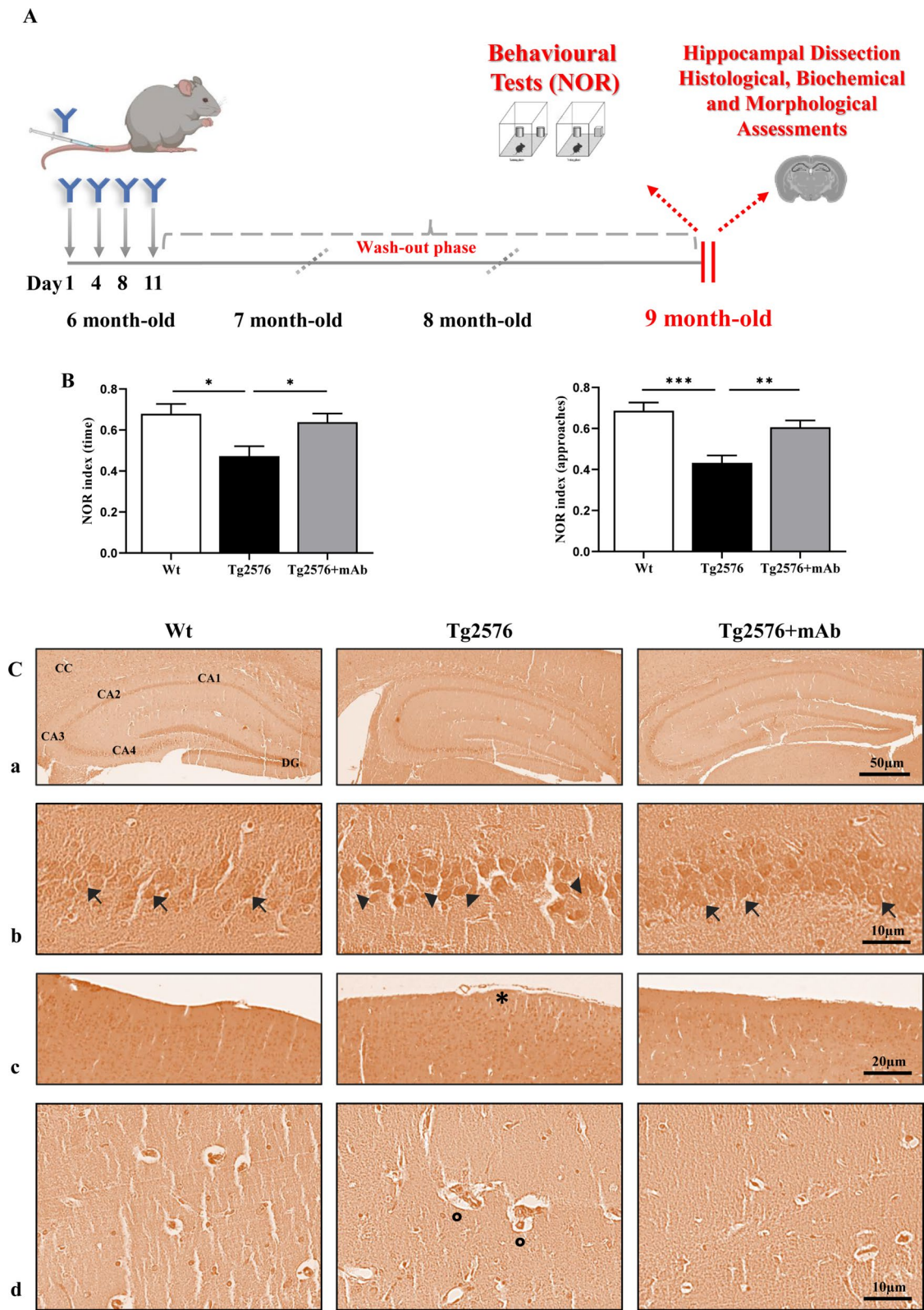
The concentration of i.v. delivered anti-tau 12 A12 mAb in TBS extracts was measured according to [40] with

some modifications. ELISA (Enzyme-Linked Immunosorbent Assay) was performed by immobilization

(See figure on next page.)

Fig. 1 Acute immunization of symptomatic 6-month-old Tg2576 mice with 12 A12 mAb mitigates the memory deficits in a sustained manner.

A Scheme of experimental design and procedures. **B** The cognitive effect of short-term administration of 12 A12 mAb in 6 month-old Tg2576 is evaluated in Novel Object Recognition (NOR) test when mice reach 9 months of age ($n = 10$ animals per each group, 5 males and 5 females for each experimental condition). Histograms show the NOR index of investigation time (left) and approaches (right) during the test trial. $p < 0.05$ is accepted as statistically significant (one-way ANOVA followed by Turkey's post-hoc test for multiple comparison among more than two groups * $p < 0.05$; ** $p < 0.01$; *** $p < 0.0005$; **** $p < 0.0001$). **C** Hematoxylin and Eosin stainings of coronal brain sections ($n = 4$ animals per each group, 2 males and 2 females for each experimental condition) from animals of all three experimental groups. Photomicrographs captured at 4X, 20X, 10X magnifications highlight: the cerebral cortex (CC) and the C-shaped structure of hippocampus with CA1-CA4 and DG regions (panel a); the layer of CA3 pyramidal neurons (panel b); the meningeal and subcortical regions (panel c and d respectively). Scale bar = 50, 20, 10 μ m



of synthetic NH₂26-44aa on the plate (being the minimal AD-relevant active moiety of the parental longer NH₂26-230) used as catching antigenic peptide [41–43]. In detail, clear 96 well high-binding plates were coated (50 µl/well) with 5 µg/ml of synthetic NH₂26-44aa in coating buffer (0.05M Carbonate-Bicarbonate, pH 9.6) o.n. at 4 °C. After that, wells were washed six times with PBS-T (0.025% Tween-20 in PBS), incubated for 3 h with blocking solution (2.5% milk in PBS-T) and then loaded (50 µl/well) with: 1) serial dilutions of 12 A12 mAb (250–0.1 ng/ml) used for the standard curve; 2) TBS extracts (diluted 5/50, 12.5/50, 25/50) or 3) blank, all prepared in blocking solution for 72 h at 4 °C. Then wells were washed six times with PBS-T and probed with 50 µl/well of mouse horseradish peroxidase-conjugated secondary antibody (715–035–151; Jackson ImmunoResearch, Baltimore; dilution 1:5000) for 1 h at room temperature. The wells were washed again six times and developed at room temperature using TMB solution (T0440; Sigma-Aldrich, Oakville, Ontario, Canada).

After blocking the reaction with 1M H₂SO₄, luminescence counts were measured for each well at 450 nm using a microplate reader (Packard TopCount, PerkinElmer, MA). For data representation, the values from individual samples were interpolated to the concentration using a second-order polynomial fit to the respective points of the standard curve and normalized amounts were expressed as pg/µg of total protein input determined by Bradford assay (BioRad).

Histopathology

Histopathological analysis of animals' hippocampi with Gill's hematoxylin n.2 (Bio-Optica, cod. 0506014) and eosin Y 1% (Bio-Optica, cod. 0510007) dye and image acquisition were carried out as previously reported [21].

Novel object recognition task (NOR task)

Three months (90 days) after the last i.v. injection, mice run the novel object recognition (NOR) task under spontaneous behavioural conditions to check the hippocampal-dependent long-term, episodic memory [44, 45]. The entire task was performed in three consecutive sessions during the same day (1-day version), according to previously published protocol [41]. In detail, during the habituation session, each mouse was placed for 10 min in the testing arena and then returned to the home-cage for 1 min interval. During the training phase, each mouse was exposed to two objects identical in size, black/white colour pattern and shape for a period of 10 min; the mouse's interest for the objects was measured by an experimenter blind to the treatment condition of the test animals as exploration, defined as both time and approaches number mice spent in sniffing and/or touching the objects with

nose and/or forepaws (e.g., <2 cm away from object). At the end of this session mice were brought back into their home-cage and were left undisturbed for 60 min inter-trial interval. During the test session each mouse was placed for 5 min in the testing arena where one of the two objects remained unvaried (familiar object, FO) while the other one was replaced with a different one (novel object, NO). In this session, object exploration was measured as above while the interest for the NO was inferred by calculating the discrimination index (NO/FO + NO ratio), defined as time/approaches number spent exploring each object (FO or NO) divided by the total time and approaches number spent in exploring both objects. A discrimination time/approach index above 0.5 indicates a preference for the NO, below 0.5 a preference for the FO, and 0.5 no preference [44, 45]. Animals with no memory impairment spent longer time investigating the novel object, giving a discrimination index significantly different from chance level (0.5), indicating that the familiar object already exists in the animals' remembrance [46].

Tissue collection and preparation

Three months (90 days) after the last injection of 12 A12 mAb, animals from three experimental groups (wild-type, vehicle-treated Tg2576, Tg2576 + mAb) were sacrificed by intraperitoneal overdose of anesthetic, perfused transcardially with 25 ml of 0.1M ice-cold phosphate buffered saline (PBS) pH 7.4 to remove blood contamination. Brains were collected, the olfactory bulbs and cerebellum were removed, hippocampi were dissected under a dissecting microscope, snap-frozen on dry-ice and, then, stored at –80 °C until use.

For biochemical analysis, total protein extracts in RIPA buffer and protein amount quantification by Bradford assay were carried out as previously reported [20].

For morphological analysis [20–22], sacrificed animals were perfused with 4% paraformaldehyde (PFA) solution in PBS. After that, brains were carefully removed from the skull, post-fixed in 4% PFA solution in PBS o/n at 4 °C and, then, passed into 30% sucrose solution in PBS for 48–72 h until equilibration. The brains were frozen by immersion in ice-cold isopentane for 3 min before being sealed into vials and stored at –80 °C until use.

Western blot analysis and semi-quantitative densitometry

Equal amounts of protein extracts (150–300 µg) were size-fractionated by SDS-PAGE Bis–Tris gel 4–12% (Bolt, Invitrogen) according to [2, 20–22]. β-actin was used as internal control of protein loading and semi-quantitative densitometric analysis was carried out by using Image J 1.4 (<http://imagej.nih.gov/ij/>). For quantification, we measured the band intensity by using a signal in the linear range. Control for nonspecific binding of the

secondary antibodies was performed by omitting the primary antibody (Suppl. Figure 2A).

SDS-PAGE was carried out on 10–20% Tricine gels (Novex, Invitrogen) with 0.1 μ m nitrocellulose membrane for the detection of 4kDa A β monomer(s) and its products, according to [47].

The following antibodies were used:

Anti-Amyloid Precursor Protein 22 C11 (66–81aa of N-terminus) mouse APP-MAB348 Chemicon; anti-A β amyloid specific (D54D2) rabbit 8243S Cell Signaling; tau antibody (BT2) mouse MN1010 ThermoFisher Scientific; Caspase-cleaved protein (CCP) NH₂-tau antibody rabbit (D₂₅-(QGGYTMHQDQ) epitope, phosphorylation-independent state) [33, 36, 37]; Anti-Amyloid Precursor Protein, C-Terminal antibody rabbit 8717 Sigma-Aldrich; BACE-1 (61-3E7) mouse sc-33711 Santa Cruz; Anti-Amyloid β Antibody (clone W0-2) mouse MABN10 Sigma-Aldrich; anti-A β /APP protein 6E10 (4-9aa) mouse MAB1560 Chemicon; β -amyloid (1–40) (D8Q7I) Rabbit mAb 12,990 Cell Signaling; β -amyloid (1–42) (D9 A3 A) Rabbit mAb 14,974 Cell Signaling; β -amyloid (D54D2) Rabbit mAb 8243 Cell Signaling; Anti-Amyloid Oligomer Antibody (A11), $\alpha\beta$, oligomeric rabbit AB9234 Sigma-Aldrich; Anti-Amyloid Fibrils OC Antibody rabbit AB2286 Sigma-Aldrich; GlycerAldehyde-3-Phosphate DeHydrogenase (GAPDH) antibody (6 C5) mouse sc-32233, Santa Cruz; GFAP antibody (2E1) mouse sc-33673 Santa Cruz; Iba1 antibody (1022–5) mouse sc-32725 Santa Cruz; anti- β -actin antibody mouse S3062 Sigma-Aldrich; Anti-PSD95 rabbit 2507 Cell Signaling; Anti-synaptophysin antibody (D-4) mouse sc-17750 Santa Cruz; anti-syntaxin 1 mouse S1172 Sigma-Aldrich; anti-SNAP25 antibody (clone SMI 81) mouse 836,301 BioLegend; anti- α synuclein antibody (clone 42) mouse 610,786 BD Transduction Laboratories; tau antibody

Tau-1 (P[−] 189–207) (clone PC1 C6) mouse 3420 Millipore; anti-phospho tau (P⁺ Ser 396) rabbit T7319 Sigma-Aldrich; tau antibody polyclonal rabbit A0024 Dako; anti-acetylated tubulin (Clone 6-11B-1) mouse T6793 Sigma-Aldrich; anti-tyrosinated tubulin rat mAb YL1/2 Harlan Sera-Lab, Loughborough, UK; anti-mouse IgG (whole molecule)-Peroxidase antibody A4416 Sigma-Aldrich (St. Louis, MO, USA); anti-rabbit IgG (whole molecule)-Peroxidase antibody A9169 Sigma-Aldrich (St. Louis, MO, USA).

Extraction of water-soluble, low-detergent A β conformers and native Dot Blot (DB) analysis

The level of native A β aggregates was measured by Dot Blot (DB) analysis as described previously [48–52] with slight modifications. Briefly, hippocampi were weighted and transferred to 4 vol ice-cold low-detergent buffer containing protease inhibitors (see above) to extract water-soluble A β oligomers. After centrifugation at 100 000 g for 1 h at 4°C, 0.5–1 μ g of the supernatants was spotted on a nitrocellulose membrane 0.22 μ m, blocked in 5% non-fat dry milk in PBS-T buffer (0.025% Tween 20 in PBS) then incubated with anti-A β amyloid specific (D54D2) (diluted 1:2000), anti-Amyloid Oligomer Antibody (A11) (diluted 1:2000), anti-Amyloid Fibrils OC Antibody (diluted 1:2000), o.n. at 4 °C. The 0.5–1 μ g amount of homogenates loaded on DB spots was established upon serial dilution curves of samples preliminarily performed to avoid saturating condition of immunodetection. The bound of primary antibodies was then probed using the appropriate HRP-conjugated secondary antibodies (Sigma-Aldrich, diluted 1:20.000) for 1 h. The blots were developed by using the enhanced chemiluminescence western blotting immunodetection system (ECL) (Thermo Fisher Scientific Waltham, MA,

(See figure on next page.)

Fig. 2 The expression level of NH₂tau does not reemerge into hippocampus from 9-month-old Tg2576 mice following anticipated and discontinuous administration of 12 A12 mAb. **A–C** Representative images of Western blotting analysis (n = 8 animals per each group, 4 males and 4 females for each experimental condition) carried out on whole protein lysates of hippocampi from animals of three experimental groups (littermate wild-type, vehicle-treated Tg2576, Tg2576 + mAb) with pan-tau BT2 antibody directed against the 194–198aa of full-length protein and with caspase-cleaved protein (CCP)-NH₂tau antiserum (D₂₅-(QGGYTMHQDQ) epitope) [36, 37] to detect the steady-state expression level of the 20–22kDa neurotoxic NH₂tau peptide, as indicated alongside the blots. Arrows on the right side indicate the molecular weight (kDa) of bands calculated from migration of standard proteins. (B–D) Histograms show the semi-quantitative densitometry of the intensity signals in immunoreactivity bands by normalization with β -actin level used as loading control. $p < 0.05$ is accepted as statistically significant (one-way ANOVA followed by Bonferroni's post-hoc test for multiple comparison among more than two groups * $p < 0.05$; ** $p < 0.01$; *** $p < 0.0005$; **** $p < 0.0001$). **E** Representative images of immunofluorescence analysis (20X) showing the increase in the punctate dot-like staining of the NH₂tau (green channel) in CA3 hippocampus from Tg2576 mice in comparison with age-matched controls and its significant downregulation following 12 A12 mAb immunization (n = 6 animals per each group, 3 males and 3 females for each experimental condition). Nuclei were counterstained with DAPI (blue channel) Scale bar = 50 μ m. Inserts at high magnification show that the fine, granular CCP-NH₂tau labeling in 9-month-old Tg2576 mice is mainly localized into the cell bodies (arrows). Scale bar = 30 μ m. **F** Fluorescence intensity quantification of the NH₂tau staining in CA3 area from three experimental groups (sample size: analyzed neurons/animal = 1020, n = 5). Values are from at least three independent experiments and statistically significant differences were calculated by one-way ANOVA followed by Bonferroni's post-hoc test for multiple comparison among more than two groups. $p < 0.05$ was accepted as statistically significant

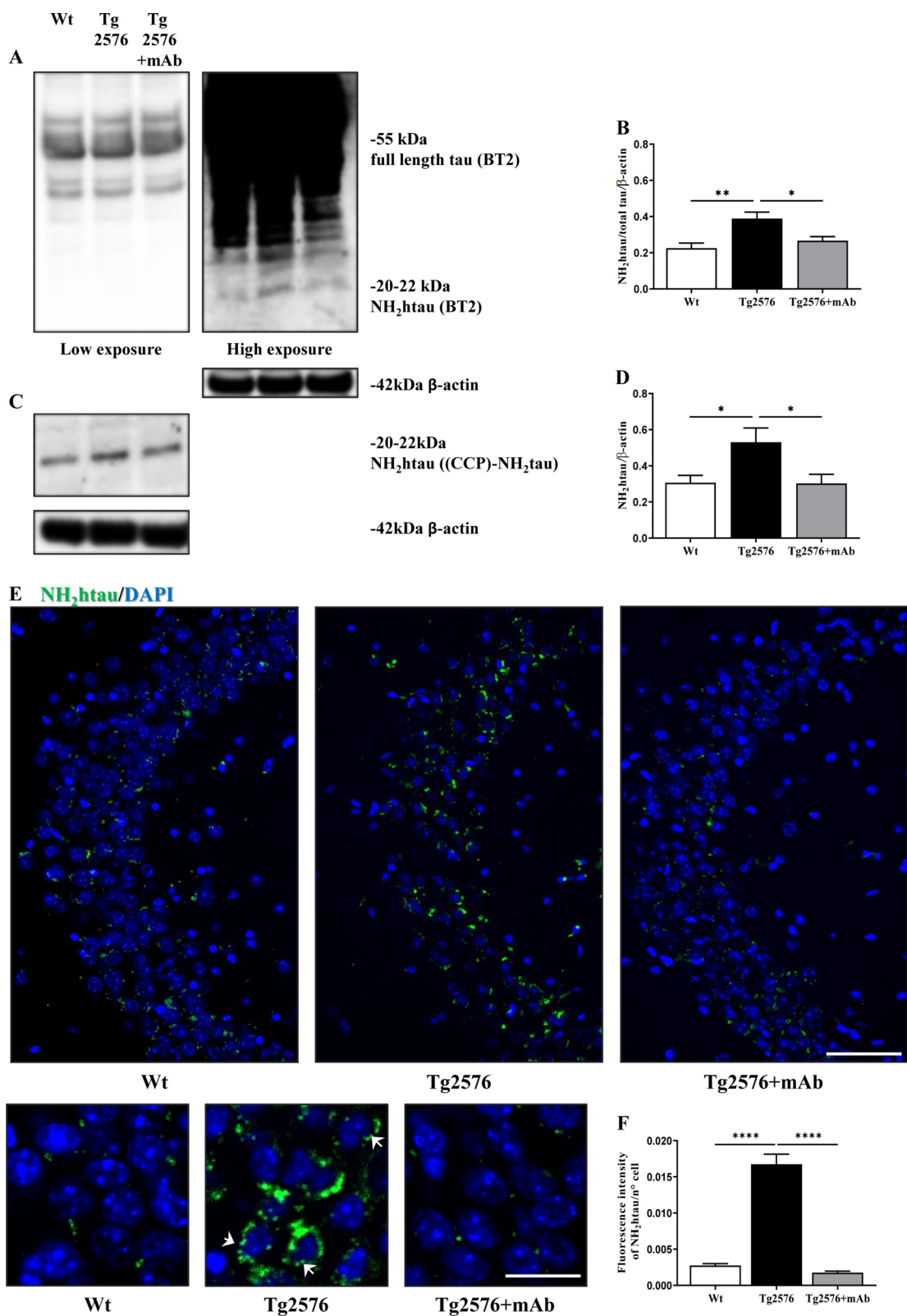


Fig. 2 (See legend on previous page.)

USA West Pico Plus, USA; Amersham Prime, Arlington Heights, IL, USA). The signal detection was performed by using the iBright Imaging Systems (Thermo Fisher Scientific). For statistical analysis, normalization was carried out by using GAPDH as internal control of protein loading. GAPDH normalization was confirmed by WB analysis of β -actin on the same samples.

Soluble and insoluble subcellular fractions for analysis of A β

Sequential extraction of A β pools with different solubility was carried out according to standard protocol [26]. Frozen hippocampi ($n = 6$ /experimental group) were weighed, homogenized in ice-cold TBS (Tris HCl 20 mM, NaCl 150 mM, pH 7.4, v/w 2:1) plus proteases inhibitor cocktail (Sigma-Aldrich, P8340) and phosphatase inhibitor cocktail (Sigma-Aldrich, P5726/P2850) and ultracentrifuged in a TLA 100.4 Rotor (Beckman Coulter) at 65,000 rpm and 4 °C for 60 min. The supernatant (called TBS extract) was collected and stored at -80 °C whereas the pellet was re-homogenized in TBS containing 1% Triton X-100 (v/w 2:1) plus proteases and phosphatase inhibitor cocktails and spun as above. The resultant supernatant (called TBS-TX extract) was collected and stored at -80 °C whereas the pellet was re-homogenized in 2% SDS (v/w 2:1) plus proteases and phosphatase inhibitor cocktails and spun as above; the resultant supernatant (SDS extract) was aliquoted and stored at -80 °C. The remaining pellet was re-homogenized in 70% Formic Acid, recentrifuged and the resulting supernatant (called FA extract) was collected and stored at -80 °C. The formic acid extract was neutralized with 1N NaOH before use for each assay. The protein amount was determined by Bradford assay (Protein Assay Dye Reagent Concentrate, Bio-Rad, Hercules, CA, United States).

Immunofluorescence assays

For immunofluorescence assays, frozen brains were mounted on cryostat (Laica CM1860 UV) by using an embedding media (OCT) and hippocampal free-floating coronal Sects. (14 μ m thickness) were obtained, according to the guidelines of Allen brain Atlas (<https://portal.brain-map.org/anatomy>). After three washes in PBS, the sections were exposed to quenching (50 mM NH₄Cl, 5 min), antigen retrieval (0.25% trypsin in PBS solution, 5 min) and blocking/permeabilizing (10% NGS, 5% BSA, and 0.5% Triton X 100 in PBS, 6 h) steps, all at room temperature and probed o.n. at 4 °C with primary antibodies (caspase-cleaved protein (CCP, NH₂-tau antiserum (D₂₅-(QGGYTMHQDQ) epitope, phosphorylation-independent state dil: 1:100; anti-A β oligomeric (A11) rabbit AHB0052 ThermoFisher Scientific, dil:1:1000; anti-Iba1 rabbit 019-19741 Wako,

dil. 1:2000) in PBS buffer containing 5% NGS, 2.5% BSA and 0.3% Triton X 100. After three washes in PBS buffer with 0.1% Triton X 100, the sections were incubated for 2 h at room temperature with the secondary antibody (goat anti-rabbit, 488, Jackson ImmunoResearch, Europe Ltd., Suffolk, UK) diluted 1:500 in PBS buffer containing 2.5% NGS, 1.25% BSA and 0.15% Triton X 100. After three washes in PBS, slices ($n = 3$) were placed on positively charged slides (Bio-Optica, Milan, Italy) and, then, nuclei counterstaining was performed by using fluoroshield mounting medium with DAPI (F6057, Sigma-Aldrich, St. Louis, MO, USA). Images (20X) are representative of at least three independent experiments and were acquired with spinning disk system for fast fluorescence confocal microscopy, with led or laser light source—Crest Optics, (Crisel Instruments, Rome, Italy). The acquisition settings for laser power and detector gain were standardized for each analyzed marker and applied throughout the study. Boundaries and subdivisions of the brain structures were identified according to the Paxinos' Mouse Brain Atlas [53]. Olympus Confocal Microscope Quantitative image analysis was performed by using Metamorph Research Imaging and ImageJ 1.4 software¹. Control for nonspecific binding of the secondary antibody was performed by omitting the primary antibody (Suppl. Figure 2B).

Data management and statistical analysis

Values were expressed as means \pm standard error of the mean (S.E.M.). Statistically significant differences were calculated by one-way analysis of variance (ANOVA) followed by Turkey's or Bonferroni's post-hoc test for multiple comparisons among more than two groups and by two-tailed unpaired t test for comparison between two different groups. $p < 0.05$ was accepted as statistically significant (* $p < 0.05$; ** $p < 0.01$; *** $p < 0.0005$; **** $p < 0.0001$). Sample size was estimated on the basis of our previously published experiments (Latina et al., 2023a-b) reporting changes in Tg2576 mice and age-matched wild-type littermate mice after 12 A12 mAb immunization. An "a priori" estimation to compute the required sample size by a given α power and effect size was carried out by G*Power statistical power analysis (version 3.1.9.4). Differences among the compared means $\geq 30\%$ with SD $\leq 20\%$ of the mean within groups have been considered to obtain a power of at least 80% with an alpha level of 0.05. All statistical analyses were performed using GraphPad Prism 8 software.

Results

Acute treatment of symptomatic 6-month-old Tg2576 mice with 12 A12 mAb leads to long-term improvement on hippocampal-dependent learning and memory deficits

In order to investigate whether the beneficial effect of 14 days immunization with 12 A12 mAb in symptomatic, 6-month-old (before amyloidosis onset) Tg2576 APP/A β mouse model could last far beyond the period of treatment (discontinuous regimen), mice of the three experimental groups (littermate wild-type, vehicle-treated Tg2576, Tg2576 + mAb) were aged for additional 3 months and, then, analyzed for recognition memory performance in Novel Object Recognition (NOR) test when they reach 9 months of age at moderate/severe stage of pathology (Fig. 1A).

The NOR test (also called one-trial discrimination test) is a well-established paradigm based on the spontaneous exploratory behaviour of rodents [44, 46, 54] towards novel stimuli. This task was chosen because it: (i) is considered the rodent equivalent of human declarative (episodic) memory involving hippocampus [55] whose progressive deterioration leads to memory deficits of AD; (ii) is ethologically relevant without external motivation, reward, punishment or extensive training [44, 45]; (iii) is largely used in numerous preclinical research studies to evaluate the cognitive performance of aging Tg2576 mice [56, 57] following passive immunization with different candidate antibodies targeting into the brain the pathogenetic species of A β and tau [58–60], including 12 A12 mAb [2].

In details, mice are challenged to discriminate between two objects on the right and left sides of the arena and the preference for a novel object means that presentation of the familiar object already exists in animals' memory [46]. The retention score was expressed with two different measures/indices, including: (1) the time ratio (time spent exploring novel object/time spent exploring both objects) [44]; (2) the discrimination index (novel object exploration – familiar object exploration)/total object exploration [45]. During the trial phase, the overall preference for both objects did not differ among all the animal cohorts (two-way ANOVA followed by Turkey's post-hoc test; $p > 0.9999$), regardless of their genotype (data not shown). On the contrary, in the test phase (Fig. 1B), when one of the two similar objects was replaced with a novel one, we found out that both time and approaches spent to investigate the novel object rather than the familiar one were significantly lower in Tg2576 mice when compared to age-matched wild-type indicating their poor performance in recognition memory (one-way ANOVA followed by Turkey's post-hoc test; *** $p < 0.0005$; * $p < 0.05$; Tg2576 versus wild-type). Remarkably, the cognitive impairment was significantly

recovered in Tg2576 mice following discontinuous delivery of 12 A12 mAb as demonstrated by their preferential exploration of the novel object in comparison to their not-immunized, age-matched counterpart (one-way ANOVA followed by Turkey's post-hoc test; ** $p < 0.01$; * $p < 0.05$ Tg2576 + mAb versus Tg2576). Notably, no improvement on cognitive performance was found in this strain following delivery of nonspecific mouse IgG (normal mouse IgG, Santa Cruz sc-2025 administered at the same dosage and period of time), ruling out the possibility of off-target effect of discontinuous passive immunization regimen (30 μ g/dose, two weekly injections on two alternate days at 6-months of age followed by 3 months of washout) on animals' performance, as we reported [2].

After that, to search for biological correlate(s) of the beneficial effect offered by discontinuous administration with 12 A12 mAb on cognitive performance, Hematoxylin and Eosin (H&E) stainings (Fig. 1C) were performed on coronal hippocampal sections from three cohorts of animals. This brain area was chosen because it: (i) plays a major role in learning and memory processes [61, 62]; (ii) is causally associated with early cognitive decline in the development of AD undergoing age-dependent structural and functional deterioration [63–65]; (iii) is selectively vulnerable to both A β and tau pathology [66]. In contrast to non-transgenic littermates, pyramidal neurons located in CA3 region (panel a) from saline-infused Tg2576 were degenerated, irregular in shape, dispersed and shrunken with dark eosinophilic cytoplasm and hyperchromatic pyknotic nuclei (black arrowheads). Meningeal (asterisk) and subcortical angiopathy (panel b–c) with dilated congested blood capillaries (circles) were also evident, in line with previous investigations reporting significant vascular degeneration in these aged mice at 9 months of age [67, 68] and in AD subjects [69]. On the contrary, following immunization with 12 A12 mAb, pyramidal neurons from transgenics appeared to be more uniform in size and evenly organized with oval shape, pale basophil cytoplasm surrounded by thin neuropiles and euchromatic nuclei (black arrows), just similar to those from age-matched wild-type controls, indicating that treatment was protective towards the histopathological changes of hippocampal cytoarchitecture occurring with the age in this strain. More importantly, normal meninges and blood vessels with no signs of microhemorrhages were detected in transgenic mice following 12 A12 mAb injection, providing the feasibility of this immunization regimen in the absence of unwanted adverse effects.

Taken together, these results show that immunization of 6-month-old (at “pre-plaque” stage) Tg2576 mice with only 4 doses of 12 A12 mAb sustains hippocampal-dependent cognitive and neuropathological improvement

approximately up to 3 months after its discontinuous administration in the absence of potential side effects.

The level of NH₂htau is reduced in hippocampus of 9-month-old Tg2576 mice beyond the period of discontinuous immunization with 4 doses of 12 A12 mAb.

To determinate the causal relationship between improved cognition and the hippocampal amount of the 12 A12 mAb-targeted NH₂htau under these experimental conditions (14 days of treatment with antibody at 6-months of age followed by 3 months of washout), Western blotting analyses followed by semi-quantitative densitometry were carried out on total protein homogenates by probing with BT2, a specific commercial tau antibody reacting against the N-terminal end of tau (194-198aa).

As shown in Fig. 2A, B, we found that the endogenous steady-state expression level of the toxic NH₂htau peptide was significantly increased in samples from 9-month-old Tg2576 mice in comparison to their littermate wild-type controls (one-way ANOVA followed by Bonferroni's post-hoc test; $^{**}p < 0.01$ Tg2576 versus wild-type), in line with our previous findings reporting its continual accumulation in this strain with aging [2]. Notably, despite the administration of the brain-penetrating 12 A12 mAb had been interrupted long before and its hippocampal retention was nearly undetectable at 3 months post-injection (Suppl.Fig. 1B–D), the N-terminal tau truncation with generation of this toxic peptide did not reappear beyond the period of discontinuous immunization, being lower in Tg2576 mice when compared to their not-immunized, age-matched counterpart (one-way ANOVA followed by Bonferroni's post-hoc test; $^{*}p < 0.05$ Tg2576 + mAb versus Tg2576). Similar results were found (one-way ANOVA followed by Bonferroni's post-hoc test; $^{*}p < 0.05$ Tg2576 versus wild-type; Tg2576 + mAb versus Tg2576) by probing with the specific Caspase-Cleaved Protein (CCP)-NH₂tau (D₂₅-(QGGYTMHQDQ epitope, phosphorylation-independent state) [36, 37], an affinity-purified antiserum specifically recognizing the toxic NH₂htau in this strain [21], just as in human brains [36].

Likewise, immunofluorescence analysis (Fig. 2E, F) with the CCP-NH₂tau antibody showed that a diffuse and dot-like cytoplasmatic staining, sometimes accumulating in ring-like perinuclear clusters, was markedly increased in CA3 hippocampus from Tg2576 mice in comparison to their wild-type controls (one-way ANOVA followed by Bonferroni's post-hoc test; $^{***}p < 0.0001$ Tg2576 versus wild-type). This finding is in agreement with our previous in vitro and in vivo

evidence demonstrating that, under pathological conditions, N-truncated tau fragment mislocalizes from neuronal axonal compartment into the soma and does not decorate microtubules, just as expected for its full length physiological counterpart. Importantly, following 12 A12 mAb treatment, the punctate positive labeling was greatly reduced (one-way ANOVA followed by Bonferroni's post-hoc test; $^{***}p < 0.0001$ Tg2576 + mAb versus Tg2576), corroborating that deleterious N-terminal tau cleavage did not re-emerge into the hippocampus of Tg2576 in spite of the anticipated interruption of antibody delivery.

Collectively, these results show that early transient immunodepletion of the NH₂htau by acute administration of 12 A12 mAb [2, 21, 22] in 6-month-old Tg2576 mice is sufficient to prevent its further increase at more late stage of pathology (when animals reach the age of 9 months), suggesting that the gradual generation of this pathogenic post-translational modification of tau in this APP-overexpressing strain develops along self-sustaining and, conceivably, A β -dependent signaling(s).

3.3 Short-term treatment with 12 A12 mAb at pre-plaque stage of Tg2576 mice reduces the on-pathway fibril aggregation of A β by attenuating the accumulation of the most toxic soluble A11-positive prefibrillar oligomers

Tg2576 mice show a long prodromal stage of cerebral β -amyloidogenesis (from 6 to 10 months) characterized by a progressive increase in the brain levels of soluble, detergent-dispersible A β with the occurrence of proteopathic seeds developing into insoluble diffuse plaques of amyloid deposits that are clearly discernable only from 12 to 15 months of age onwards [27]. Compelling evidence in in vitro systems and in vivo AD animal models and in humans have shown that soluble pathogenetic species of both tau and A β act in a cooperative and/or synergic way, indicating the possibility that a close interplay between these two toxic forms is more likely to be the main contributor to full-blown clinical trajectory in AD development [16, 70]. Therefore, since the acute immunization with 12 A12 mAb coincides with the "lag phase" of A β amyloidosis starting in this animal model approximately at 6 months of age, we set about to investigate whether treatment with this anti-tau antibody could also indirectly impact on the time-dependent A β accumulation and/or aggregation. To this aim, whole hippocampal lysates from 9-month-old animals of three experimental groups (littermate wild-type, vehicle-treated Tg2576, Tg2576 + mAb) were evaluated by Western blotting with WO2 and 6E10, two independent commercial monoclonal APP/A β antibodies against the N-terminal end of

human A β peptide (1-16aa) routinely used on brain samples from AD subjects, Tg2576 mice and other preclinical APP/A β mouse models [71, 72]. As shown following semi-quantitative densitometry analysis (Fig. 3A–D), a significant increment in the immunoreactivity level of A β was detected in Tg2576 mice when compared to wild-type littermates (one-way ANOVA followed by Bonferroni's post-hoc test; *** p < 0.0005; ** p < 0.01 Tg2576 versus wild-type), consistent with previous investigations [2, 27, 73, 74]. Remarkably, the intensity signal of 4 kDa band turned out to be significantly upregulated in 12 A12 mAb-treated Tg2576 mice (one-way ANOVA followed by Bonferroni's post-hoc test; ** p < 0.01; * p < 0.05 Tg2576 versus wild-type), in keeping with animals' improved behavioural performance when compared to their not-immunized age-matched counterpart (Fig. 1B).

To corroborate these findings, hippocampal extracts were next probed with D54D2, a commercial monoclonal A β -specific antibody that reacts against the N-terminal (human-specific) epitope of A β without any crossreaction with APP full length [21, 22, 75, 76]. As shown in Fig. 4A, B, a marked elevation in immunoreactivity of bands corresponding to human monomeric A β 4 kDa (1 mer) and its trimeric 12 kDa oligomeric assemblies (3 mer) was detected in 9-month-old Tg2576 mice when compared to wild-type controls (one-way ANOVA followed by Bonferroni's post-hoc test; **** p < 0.0001; ** p < 0.01 Tg2576 versus wild-type), in agreement with age-dependent accumulation of D54D2-positive multiple A β species occurring in this strain [21, 22, 75, 77]. Again, we found out that treatment with 12 A12 mAb significantly upregulated the intensity signal of 1 mer 4 kDa in Tg2576 mice (one-way ANOVA followed by Bonferroni's post-hoc test; **** p < 0.0001 Tg2576 + mAb versus Tg2576) with a concomitant inverse reduction of the corresponding 3 mer 12 kDa form (one-way ANOVA followed by Bonferroni's post-hoc test; * p < 0.05 Tg2576 + mAb versus Tg2576). Finally, a similar trend (Fig. 4B–E) was also obtained by probing with two independent commercial monoclonal antibodies, D9 A3 A and the D8Q7I that selectively recognize the A β 42 and A β 40 C-terminal neo-epitope, respectively [51, 52, 77]. Interestingly, we observed that, just as for 6E10 and

WO2 APP/A β antibodies, the immunoreactivity levels of 1 mer 4 kDa detected both A β -specific antibodies were higher in 12 A12 mAb-treated Tg2576 in comparison to their not-immunized counterpart (one-way ANOVA followed by Bonferroni's post-hoc test; **** p < 0.0001 Tg2576 + mAb versus Tg2576) but that the trend of D8Q7I did not reach statistical significance (ns = not significant), suggesting that the largest part of soluble A β species present into animals' hippocampi following treatment 12 A12 mAb is more likely to consist of monomeric A β 42 peptide.

To better investigate the changes in the aggregation profile of A β burden under our experimental conditions, the A β assemblies from water-soluble, low-detergent tissue fractions of each experimental groups were measured and characterized under non-denaturing conditions by native dot-blot with OC and A11 antibodies. In particular, the A11 and OC conformation-selective, stage-dependent A β antibodies do not recognize monomers but identify in this strain two distinct classes of transient conformers (prefibrillar and fibrillar oligomers, respectively) characterized by mutually exclusive structural epitopes that sequentially manifest at different times before the fibril generation and nearly disappear after Congo red-positive amyloid plaques have been formed [49, 51, 52, 78]. As shown in Fig. 5A–D, Tg2576 mice accumulated the A11-positive non-fibrillar A β oligomers to a greater extent than the OC-immunoreactive fibrillar ones when compared to their age-matched non-transgenic littermates (one-way ANOVA followed by Bonferroni's post-hoc test; *** p < 0.0005 Tg2576 versus wild-type), confirming that in this strain at 9 months of age the prevailing prefibrillar (A11 positive) assemblies are only poorly stained by OC antibody (one-way ANOVA followed by Bonferroni's post-hoc test; p > 0.9999; among all the three experimental groups). These findings are in agreement with previous studies reporting that a strong signal as detected by OC antibody emerges in this strain only after 12–15 months of age during the plaques maturation when parenchymal deposition of insoluble A β aggregates starts [51, 52, 79]. Interestingly, a significant decline in level of A11-immunoreactive signal was discernable in transgenic animals following

(See figure on next page.)

Fig. 3 Tg2576 mice immunized with 12 A12 mAb (only 4 doses) at 6 months of age show significantly high level of 4 kDa A β monomer up to 12 week post-injection in correlation with their improved cognitive performance. **A,C** Representative images of Western blotting analysis (n = 6 animals per each group, 3 males and 3 females for each experimental condition) carried out on whole protein lysates of hippocampi from animals of three experimental groups (littermate wild-type, vehicle-treated Tg2576, Tg2576 + mAb) with two APP/A β antibodies WO2 (4-10aa of human A β peptide) and 6E10 (1-16aa of human A β peptide), as indicated alongside the blots. Arrows on the right side indicate the molecular weight (kDa) of bands calculated from migration of standard proteins. **B,D** Histograms show the semi-quantitative densitometry of the intensity signals in immunoreactivity band of 4 kDa peptide(s) by normalization with β -actin level used as loading control. Notice that the expression level of APP full length does not change following immunization with 12 A12 mAb. p < 0.05 is accepted as statistically significant (one-way ANOVA followed by Bonferroni's post-hoc test for multiple comparison among more than two groups * p < 0.05; ** p < 0.01; *** p < 0.0005; **** p < 0.0001)

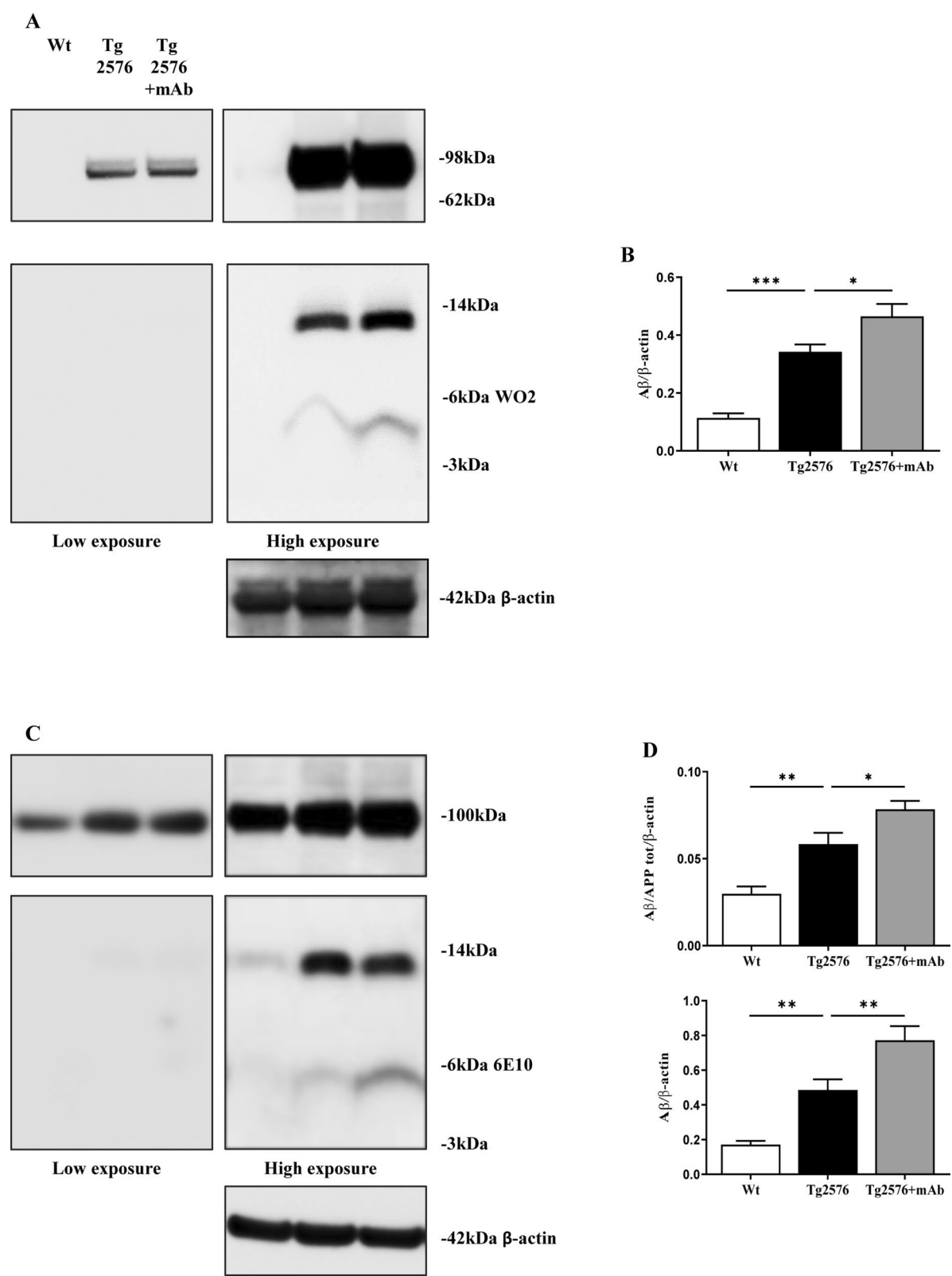


Fig. 3 (See legend on previous page.)

immunization with 12 A12 mAb (one-way ANOVA followed by Bonferroni's post-hoc test; $**p < 0.01$ Tg2576 + mAb versus Tg2576) whereas no reciprocal change was contextually in intensity of OC antibody (one-way ANOVA followed by Bonferroni's post-hoc test; $p > 0.9999$; among all the three experimental groups). Finally, native immunoblotting with D54D2 antibody followed by semiquantitative densitometry using GAPDH as internal control (Fig. 5E, F) confirmed the signal pattern detected under denaturing conditions with D54D2 and D9 A3 A (compare Fig. 5E, F with Fig. 4A, B), indicating that the changes in A11 and OC immunoreactivity actually arose from oligomers of 1 mer 4kDa A β peptide.

To better characterize the conformation(s) of A β oligomers, coronal hippocampal sections were analyzed by immunofluorescence with A11 antibody (Fig. 6A, B). A striking increase in A11 immunoreactivity was detected in CA3 hippocampus of Tg2576 with diffuse pattern appearing mainly in intracellular granular structures when compared with wild-type littermates (one-way ANOVA followed by Bonferroni's post-hoc test; $****p < 0.0001$ Tg2576 versus wild-type). As in other AD models [50, 80, 81], the staining, intracellular rather than extracellular, developed by A11 (Kayed et al., 2007) in hippocampal layers was detected mostly distributed around the nucleus and along the neuritic processes. This finding is in line with previous studies showing that A β oligomers initially accumulate inside the neurons and only at later stage of neuropathology, upon secretion, aggregate into extracellular fibrils [81, 82]. Consistent with the trend of dot-blot reports above (Fig. 5A, B), the fluorescent signals were decreased in transgenic mice following 12 A2 mAb treatment, indicating that immunization reduces the intracellular A11-positive A β oligomeric deposits in CA3 neurons (one-way ANOVA followed by Bonferroni's post-hoc test; $****p < 0.0001$ Tg2576 + mAb versus Tg2576).

In order to evaluate the effect of 12 A12 mAb on the distribution of different A β species according to their solubility, we took advantage of a multi-step ultracentrifugation fractionation protocol largely used to extract distinct pools of A β with different aggregation properties from

both AD and Tg2576 brains [26]. Hippocampi from the three different experimental groups were fractionated by means of sequential extraction to recover four fractions: (i) the water-soluble (TBS extract, extracellular soluble A β), (ii) the detergent-soluble (TBST extract, intracellular A β), (iii) the SDS-stable (SDS extract, membrane-associated A β) and (iv) the 70% Formic Acid-soluble (FA extract, plaque-associated extracellular insoluble A β) [26]. The amounts of total A β recovered from soluble (SDS extract) and insoluble (FA extract) fractions were analyzed by Western Blotting with D54D2 antibody followed by semiquantitative densitometry. As shown in Suppl. Fig. 3, the level of 4kDa signal band in SDS extract was higher in Tg2576 + mAb group when compared to untreated transgenics (one-way ANOVA followed by Bonferroni's post-hoc test; $****p < 0.0001$ Tg2576 + mAb versus Tg2576), indicating that 12 A12 mAb treatment increases the soluble pool of A β monomer(s) likely by interfering with the mechanism of its aggregation. In support of this finding, a diminution of 12kDa A β (SDS-stable trimer) level was contextually detected in SDS extract from Tg2576 mAb group when compared to not-immunized counterpart (one-way ANOVA followed by Bonferroni's post-hoc test; $*p < 0.05$ Tg2576 + mAb versus Tg2576). More importantly, the level of soluble A β 1–42 detected by probing with specific D9 A3 A antibody was also increased in the Tg2576 mAb group in comparison with not-immunized counterpart (one-way ANOVA followed by Bonferroni's post-hoc test; $*p < 0.05$ Tg2576 + mAb versus Tg2576), further corroborating our results on unfractionated protein extracts. On the contrary, only a faint signal for 4kDa A β was detected in FA extract in Tg2576 + mAb (one-way ANOVA followed by Bonferroni's post-hoc test; $****p < 0.0001$ Tg2576 + mAb versus Tg2576) whereas an immunoreactivity smear centered at 4 kDa (monomers) and 50–60 kDa (larger oligomers) was contextually visible in untreated transgenics.

Collectively, these biochemical results suggest that discontinuous immunization with 12 A12 mAb prevents in Tg2576 mice the formation of toxic, possibly A β 42, pre-fibrillar oligomers recognized by conformational-selective A11 antibody without promoting their contextual

(See figure on next page.)

Fig. 4 The soluble pool of 4 kDa A β detectable in 9-month old Tg2576 mice after discontinuous immunization with 12 A12 mAb mainly consists of monomeric A β 42 peptide. **A,C,E** Representative images of Western blotting analysis ($n = 8$ animals per each group, 4 males and 4 females for each experimental condition) carried out on whole protein lysates of hippocampi from animals of three experimental groups (littermate wild-type, vehicle-treated Tg2576, Tg2576 + mAb) with three A β antibodies D54D2 (N terminus of human A β), D9 A3 A and D8Q7I (the A β 42 and A β 40 C-terminal neo-epitope, respectively) as indicated alongside the blots. Arrows on the right side indicate the molecular weight (kDa) of bands calculated from migration of standard proteins. **B,D,F** Histograms show the semi-quantitative densitometry of the intensity signals in immunoreactivity band of 4kDa peptide(s) by normalization with β -actin level used as loading control. Notice the increase of 1 mer 4kDa form following immunization with 12 A12 mAb. $p < 0.05$ is accepted as statistically significant (one-way ANOVA followed by Bonferroni's post-hoc test for multiple comparison among more than two groups $*p < 0.05$; $**p < 0.01$; $***p < 0.0005$; $****p < 0.0001$)

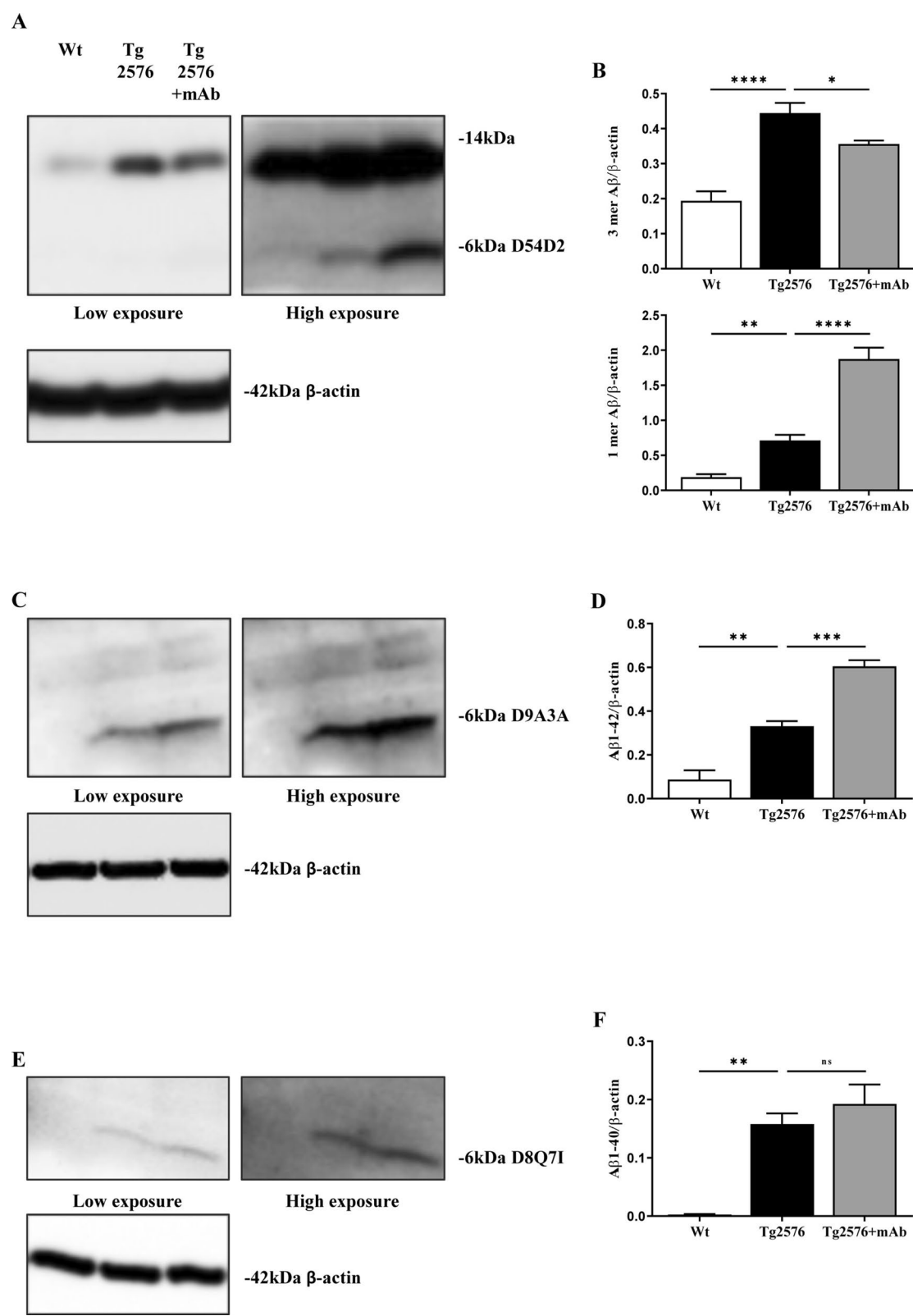


Fig. 4 (See legend on previous page.)

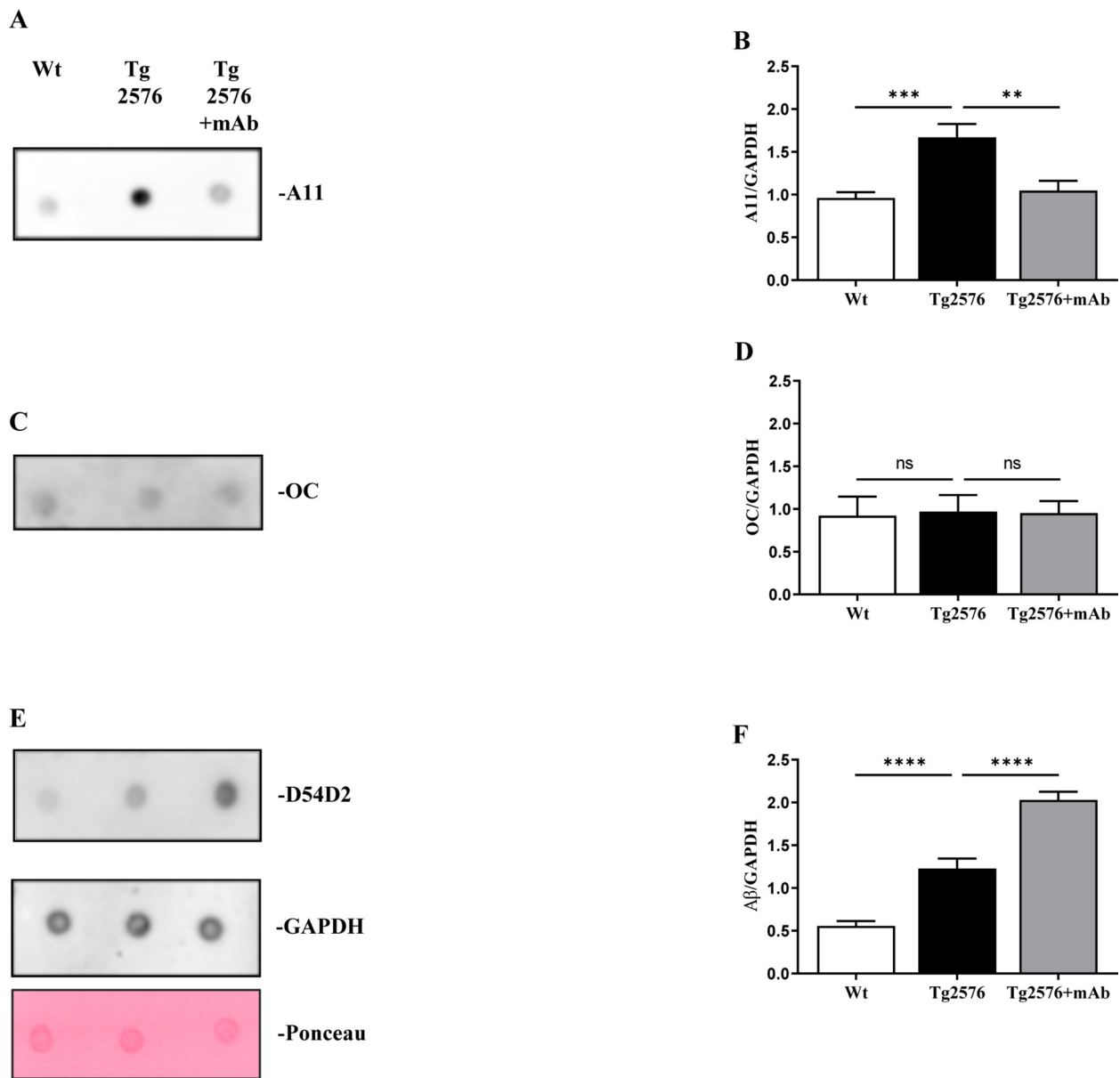


Fig. 5 Early and short-term delivery of 12 A12 mAb in symptomatic Tg2576 mice prevents later on the formation of most toxic soluble prefibrillar Aβ oligomers recognized by conformational-selective A11 antibody without promoting their contextual conversion to OC-positive fibrillar ones. **A,C,E** Native dot-blots of water-soluble Aβ conformers from hippocampi of animals (n = 6 animals per each group, 3 males and 3 females for each experimental condition) of three experimental groups (littermate wild-type, vehicle-treated Tg2576, Tg2576 + mAb) probed with the conformation-dependent antibodies A11 (specific for prefibrillar oligomers) and OC (specific for fibrillar oligomers) and with the D54D2 antibody (specific for the N-terminus of Aβ). Ponceau staining is used to visualize the overall protein amount. **B,D,F** Histograms show the semi-quantitative densitometry of the intensity signals of dots by normalization with GAPDH level used as loading control. $p < 0.05$ is accepted as statistically significant (one-way ANOVA followed by Bonferroni's post-hoc test for multiple comparisons among more than two groups. * $p < 0.05$; ** $p < 0.01$; *** $p < 0.0005$; **** $p < 0.0001$)

conversion to OC-positive fibrillar ones. This suggests that 12 A12 mAb might sustain a therapeutic action in vivo by involving an attenuation of the on-pathway fibril aggregation of Aβ and/or an acceleration of the off-pathway non-fibril route.

12 A12 mAb treatment increases the level of less toxic Aβ monomer(s) without affecting the amyloidogenic APP processing

We have previously shown that acute (14 days) treatment with 12 A12 mAb downregulates the steady state expression levels of holoprotein APP and Beta-Secretase

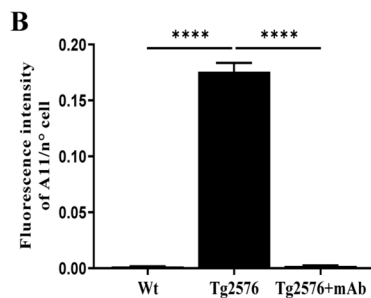
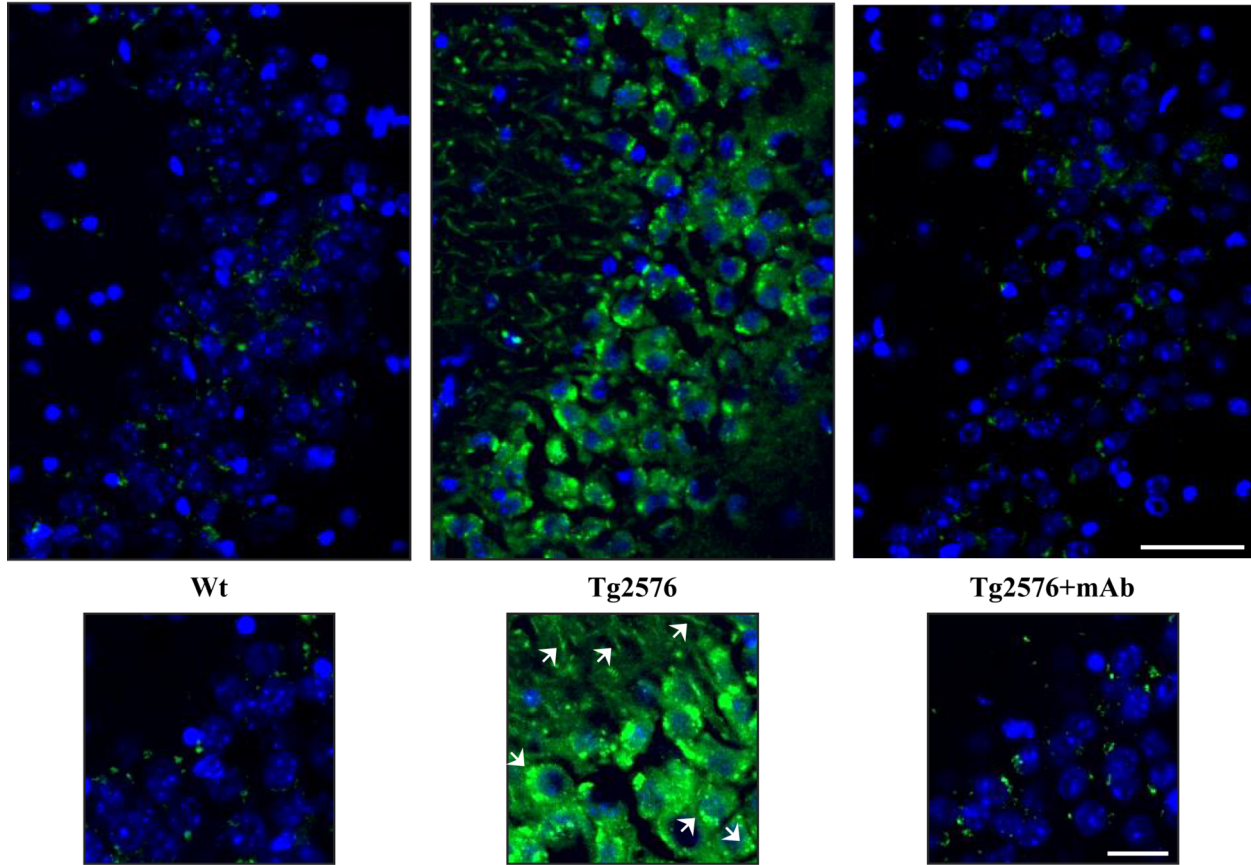
A**A11/DAPI**

Fig. 6 The intracellular load of A11-positive A β oligomers is greatly reduced into hippocampus of old Tg2576 APP/A β mouse model by preventive treatment with 12 A12 mAb. **A** Immunostaining with A11 oligomeric antibody (green channel) on coronal hippocampal sections to visualize the A β oligomers. Nuclei were counterstained with DAPI (blue channel). Representative microphotographers (20X) show the dot-like immunoreactivity differences in A11-positive neurons in CA3 layers from all three experimental groups (littermate wild-type, vehicle-treated Tg2576, Tg2576 + mAb) ($n = 4$ animals per each group, 2 males and 2 females for each experimental condition). Scale bar = 50 μ m. Inserts at high magnification show that punctate A11 labeling in Tg2576 mice is mainly localized into the cell bodies around the nucleus and along the neuritic processes (arrows). Scale bar = 20 μ m. **B** Fluorescence intensity quantification of the A11 labeling in CA3 area from three experimental groups (sample size: analyzed neurons/animal = 1250, $n = 5$). Values are from at least three independent experiments and statistically significant differences were calculated by one-way ANOVA followed by Bonferroni's post-hoc test for multiple comparisons among more than two groups. $p < 0.05$ was accepted as statistically significant. (* $p < 0.05$; ** $p < 0.01$; *** $p < 0.0005$; **** $p < 0.0001$)

1 (BACE1) with consequent reduction of the 4kDa A β production into hippocampus from 6-month-old Tg2576 mice. A probable underlying mechanism involves the coordinated modulation of the endocytic (BIN1, RIN3) and bioenergetic (glycolysis and L-Lactate) pathways [2, 21, 22]. Therefore, to get more insights into the APP/A β processing under our experimental conditions, we assessed the in vivo effect of 12 A12 mAb immunization on the expression levels of APP full length and BACE1 that directs the holoprotein APP along the amyloidogenic pathway with production of its C-terminal soluble fragment β (β -CTF or C99). To this aim, whole hippocampal lysates from 9-month-old animals of three cohorts (littermate wild-type, vehicle-treated Tg2576, Tg2576 + mAb) were evaluated by Western blotting with 22 C11 (66-81aa of N-terminus of APP) and anti-pan-C-terminal APP (751-770aa of C-terminus of APP) antibodies -recognizing the full-length APP and the C-terminal soluble products (CTFs) respectively- and with BACE1 antibody directed against the beta-site APP-cleaving endoprotease. Semiquantitative densitometric analysis of signal bands (Fig. 7A–F) showed a significant up-regulation of APP, BACE1 and C99 (β -CTF) in Tg2576 mice when compared to their non-transgenic littermates (one-way ANOVA followed by Bonferroni's post-hoc test; *** p < 0.0005; ** p < 0.01 Tg2576 versus wild-type), confirming the occurrence of a preferential activation of amyloidogenic pathway in this strain. However, despite the significant increase of 4kDa A β immunoreactivity band detected with three specific antibodies (Fig. 3–4), no significant change in the steady state expression levels of APP, BACE1 and APP C99 (β -CTF) was found in transgenic animals following immunization with 12 A12 mAb (one-way ANOVA followed by Bonferroni's post-hoc test; p > 0.9999 Tg2576 + mAb versus Tg2576). This indicates that the discontinuous regimen with 12 A12 mAb did not promote the BACE1-initiated amyloidogenic APP pathway.

Taken together these results indicate that: (i) the acute immunization with 12 A12 mAb in 6-month-old Tg2576 mice does not alter the amyloidogenic processing of APP (APP, C99, BACE1) when animals reach 9 months

of age; (ii) the great accumulation of 4kDa A β monomer detected in their hippocampi is not due to an increased production but, more likely, to 12 A12 mAb-mediated inhibitory action on its time-dependent aggregation and fibril maturation, even though an effect on clearance cannot be ruled out.

Early and transient immunoneutralization of the NH₂htau in Tg2576 mice normalizes microgliosis and synaptic derangement at more moderate/severe stage of AD pathology

Extensive microglial stimulation and synaptic alterations are tightly associated with A β deposition and tau neuropathology being the strongest predictors of cognitive impairment and dementia, both in AD models and in humans [83–85]. Therefore, Western blotting analyses followed by semi-quantitative densitometry were carried out on whole homogenates of animals' hippocampi by probing with specific antibodies for Glial Fibrillary Acidic Protein (GFAP) and Ionized calcium-Binding Adaptor molecule 1 (Iba1), two well-established markers of astrogliosis and microgliosis whose expression level respectively increase with their activated state [86–89]. Moreover, the levels of some relevant both pre- and post-synaptic proteins such as α -synuclein, Synaptosomal-Associated Protein, 25kDa (SNAP25), synaptophysin, syntaxin and PostSynaptic Density Protein 95 (PSD95) were measured.

As shown in Fig. 8A–D, the steady-state expression level of Iba1 -but not of GFAP (one-way ANOVA followed by Bonferroni's post-hoc test; p > 0.9999 among the three experimental groups)- was elevated in 9-month-old Tg2576 mice when compared to their non-transgenic littermates (one-way ANOVA followed by Bonferroni's post-hoc test; ** p < 0.01 Tg2576 versus wild-type). This is consistent with the prominent microglial activation discernible in plaque-accumulating AD strains at late stage of neuropathology [90]. Antibody treatment significantly downregulated the intensity signal of Iba1 immunoreactive band (one-way ANOVA followed by Bonferroni's post-hoc test; ** p < 0.01 Tg2576 + mAb versus Tg2576), confirming the finding that microglial activation is not

(See figure on next page.)

Fig. 7 The expression levels of full-length APP, BACE1 and β CTF are unchanged in hippocampi from 9-month-old Tg2576 mice following discontinuous immunization with 12 A12 mAb. **A,C,E** Representative images of Western blotting analysis (n = 8 animals per each group, 4 males and 4 females for each experimental condition) carried out on whole protein lysates of hippocampi from animals of three experimental groups (littermate wild-type, vehicle-treated Tg2576, Tg2576 + mAb) with 22 C11 (66-81aa of N-terminus of APP), BACE1 and anti-pan-C-terminal APP (751-770aa of C-terminus of APP) antibodies, as indicated alongside the blots. Arrows on the right side indicate the molecular weight (kDa) of bands calculated from migration of standard proteins. **B,D** Histograms show the semi-quantitative densitometry of the intensity signals in immunoreactivity bands by normalization with β -actin level used as loading control. p < 0.05 is accepted as statistically significant (one-way ANOVA followed by Bonferroni's post-hoc test for multiple comparisons among more than two groups * p < 0.05; ** p < 0.01; *** p < 0.0005; **** p < 0.0001)

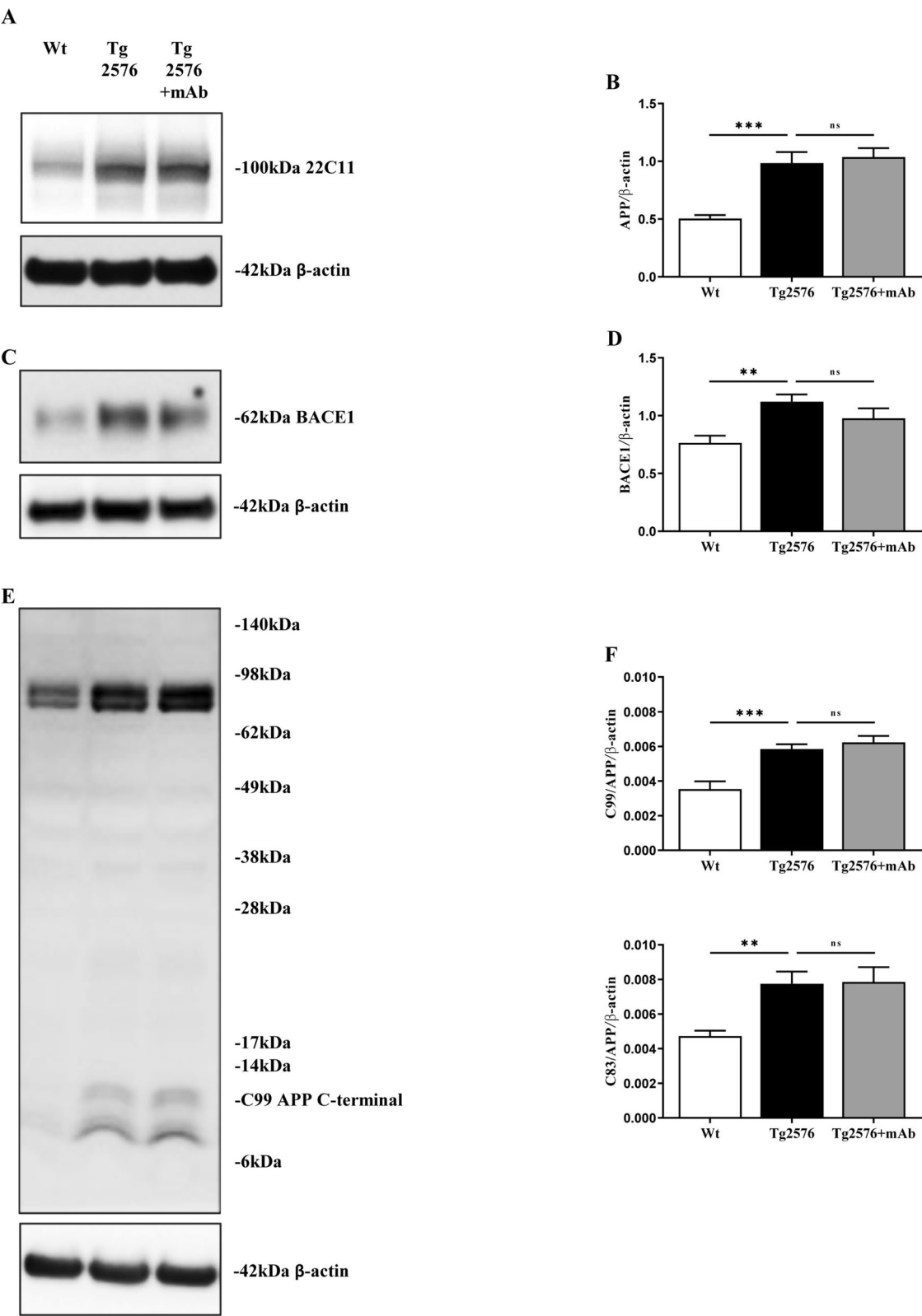


Fig. 7 (See legend on previous page.)

required for efficacy in passive immunization in Tg2576 that is not dependent on FcR-mediated phagocytic events [91–93]. These results suggest that gradual removal of tau aggregates, and an indirect clearance of A β deposits, actually reduce microgliosis and, then, are not associated with extensive gliosis.

By immunofluorescence analyses on coronal brain sections (Fig. 8E–F), we observed a striking increase in Iba-1-positive microglia immunoreactivity in CA2 parenchyma of Tg2576 hippocampi when compared to wild-type controls (one-way ANOVA followed by Bonferroni's post-hoc test; **** $p < 0.0001$ Tg2576 versus wild-type), a result in keeping with our Western Blotting analyses on the corresponding protein extracts assessing its steady-state expression levels (Fig. 8C, D). This finding is also consistent with previous studies reporting a marked microgliosis with pronounced changes in density and morphological homeostatic shapes in different AD mice models, including the current strain [94–98]. Interestingly, an increment in volume of cell body (soma) and reduction in ramification length were discernable in a small part of reactive microglial population of Tg2576 in comparison with their resting-state, not-transgenic counterpart characterized by more elongated processes and complex branching. Discontinuous immunization with 12 A2 mAb exerted an evident anti-inflammatory action (one-way ANOVA followed by Bonferroni's post-hoc test; * $p < 0.05$ Tg2576 + mAb versus Tg2576), in line with previous investigations reporting that a beneficial effect on microglia following in vivo delivery of therapeutic antibody is more likely to be secondary to its prevention of tau-mediated neurotoxicity [2, 39].

Furthermore, as shown in Fig. 9A–J, the immunoreactivity signals of PSD95, α -synuclein, SNAP25 were increased in 9 month-old Tg2576 mice (one-way ANOVA followed by Bonferroni's post-hoc test; ** $p < 0.01$ * $p < 0.05$ Tg2576 versus wild-type) whereas no significant change was contextually detected for synaptophysin and syntaxin

(one-way ANOVA followed by Bonferroni's post-hoc test; $p > 0.9999$). These results are consistent with the observation that a synaptic derangement/imbalance/remodelling, rather than an overall loss of synaptic density, takes place in AD patients and in aging Tg2576 mice [99]. Interestingly and in agreement with our behavioural results (Fig. 1), the synaptic imbalance was normalized in Tg2576 mice following short-term immunization with 12 A12 mAb, even up to baseline level of their age-matched wild-type controls (one-way ANOVA followed by Bonferroni's post-hoc test; ** $p < 0.01$; * $p < 0.05$ Tg2576 + mAb versus Tg2576).

After that, to investigate the effect of 12 A12 mAb administration on tau hyperphosphorylation and microtubule instability that also take place along with cerebral β -amyloidosis in AD development, Western blotting analyses followed by semi-quantitative densitometry were performed on hippocampal lysates from wild-type, Tg2576 and Tg2576 + mAb by probing with a panel of commercial antibodies against two key phospho-dependent epitopes of tau (PHF13 P⁺ Ser396; Tau-1 P[−] 189–207) known to reduce its affinity for microtubules, acetyl- α -tubulin (stable) and tyrosinylated- α -tubulin (instable). As shown (Suppl. Figure 4), no apparent change in the phosphorylation state of tau at the two sites analyzed was detected among the three experimental groups (one-way ANOVA followed by Bonferroni's post-hoc test; $p > 0.9999$), possibly because developmentally-regulated phospho-tau baseline is higher in this strain [25]. Although tau neuropathology appears first in this amyloidogenic model [60, 100], these findings are more in line with the notion that a marked and extensive protein hyperphosphorylation at multiple residues becomes more evident only at later stages (from 12–18 months) in concomitance with the manifestation of Congo red-positive plaques [28, 101, 102]. Consistently, neither acetyl- α -tubulin (stable) nor tyrosinylated- α -tubulin (instable) were affected (one-way ANOVA followed by Bonferroni's

(See figure on next page.)

Fig. 8 Treatment with 12 A12 mAb reduces microgliosis but does not affect astrocytes in 9-month-old Tg2576 mice. **A,C** Representative images of Western blotting analysis ($n = 8$ animals per each group, 4 males and 4 females for each experimental condition) carried out on whole protein lysates of hippocampi from animals of three experimental groups (littermate wild-type, vehicle-treated Tg2576, Tg2576 + mAb) with antibodies for GFAP, Iba1 (as indicated alongside the blots). Arrows on the right side indicate the molecular weight (kDa) of bands calculated from migration of standard proteins. **B,D** Histograms show the semi-quantitative densitometry of the intensity signals of bands by normalization with β -actin level used as loading control. $p < 0.05$ is accepted as statistically significant (one-way ANOVA followed by Bonferroni's post-hoc test for multiple comparisons among more than two groups * $p < 0.05$; ** $p < 0.01$; *** $p < 0.0005$; **** $p < 0.0001$). **E** Microphotographers (20X) of Iba1⁺-stained (green channel) microglial cells in hippocampal CA2 region from coronal sections of animals ($n = 4$ animals per each group, 2 males and 2 females for each experimental condition) of three experimental groups (littermate wild-type, vehicle-treated Tg2576, Tg2576 + mAb). Nuclei were counterstained by DAPI (blue channel). Scale bar = 20 μ m. Arrows and asterisks show large and highly ramified (homeostatic, resting state) versus small with high circularity (reactive state) microglia morphology, respectively. **F** Fluorescence intensity quantification of the Iba1 labeling in CA2 area from three experimental groups (sample size: analyzed cells/animal = 1150, $n = 5$). Values are from at least three independent experiments and statistically significant differences were calculated by one-way ANOVA followed by Bonferroni's post-hoc test for multiple comparisons among more than two groups. $p < 0.05$ was accepted as statistically significant

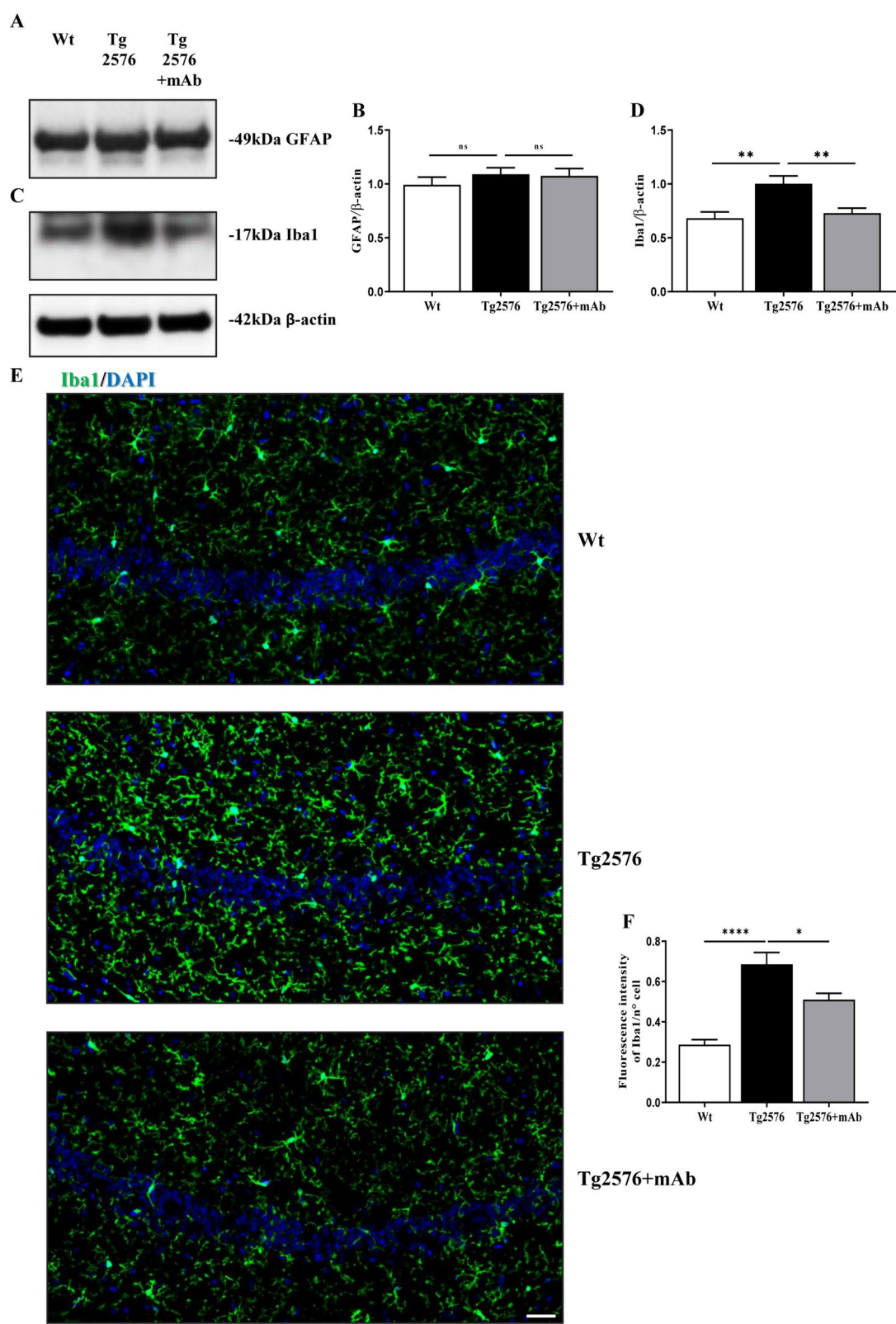


Fig. 8 (See legend on previous page.)

post-hoc test; $p > 0.9999$ among the three experimental groups) indicating that alterations in tau-dependent microtubule dynamics do not greatly contribute to AD neuropathology in Tg2576 mice at least up to 9 months of age.

Taken together, these results indicate that the long-lasting, beneficial effect of discontinuous administration of 12 A12 mAb in Tg2576 mice involves a modulation of microglia-based inflammatory response along with synaptic stabilization into their hippocampi.

Discussion

Three are the main findings of the present study: (i) short-term neutralization of pathogenetic NH_2htau following intravenous delivery of 12 A12 mAb in symptomatic 6-month-old Tg2576 APP/A β mouse model leads to durable (up to 90 days post-injection) and safe (no vascular damage, excessive microglia overactivation) protective action on hippocampal-dependent cognitive functions and associated synaptic pathology (Fig. 1,8,9); (ii) therapeutically-targetable NH_2htau early (at pre-deposit stage) synergizes with soluble forms of A β and its 12 A12 mAb-mediated depletion negatively interferes with its aggregation pathway leading in older animals to decrease of the most toxic, prefibrillar oligomers (A11-positive) formation (Fig. 5,6) with a concomitant inverse increase of its unaggregated monomeric form (Fig. 3,4), in the absence of any change of the APP expression level and its amyloidogenic processing (Fig. 7); (iii) cleavage of endogenous tau at its N-terminal region with production of neurotoxic NH_2htau does not reemerge into their hippocampi beyond the period of discontinuous immunization (Fig. 2), suggesting that this post-translational modification, once started, can't persist and/or progress over time independently of A β maturation.

Overall, our behavioural, histological, biochemical and morphological results provide additional evidence in support of the bidirectional causality between cerebral A β accumulation and tau neuropathology as main driver of the AD continuum [14, 16, 18] (Fig. 10), advocating for the development of multi-targeted approaches with additive and/or synergistic therapeutic efficacy to halt its progression [3, 103]. By showing for the first time that

discontinuous immunization with 12 A12 mAb has an impact on cerebral A β amyloidosis at “pre-plaque” stage (i.e. during the “lag phase” of amyloid aggregation), this study extends previous *in vivo* investigations reporting that both active [90] and passive immunization [60, 104–106] against the neurotoxic species of tau, in particular those encompass the protein's N-terminal domain, significantly ameliorates the “pre-established” A β pathology (i.e. at post-deposit stage) in different lines of APP/A β -expressing AD mouse models. To this point, it's noteworthy that the “accumulation hypothesis” posits that the plaques load in APP-overexpressing Tg2576 [107] reflects the cumulative small excess of A β production over its clearance that amasses in a time-dependent manner. Indeed, the deposition of A β into insoluble plaque -that typically starts at 10–11 months of age in this strain and progresses onwards up to 23 months- is anticipated by a slow and critical seeding mechanism from 6 to 10 months (aggregation in oligomers and intermediate protofibrils with a sigmoidal kinetic) followed by a more rapid fibrillogenesis into mature fibers [26, 27]. Once the nuclei have formed, addition of extra A β monomers becomes thermodynamically favourable resulting in fast growth. Therefore, it is conceivable that agents that intercept the nucleation of A β in the initial stages of seeding when the nuclei are unstable can block its further maturation. In this framework, in line with the notion that soluble A β pool has to accumulate (and oligomerize) to a threshold level before plaques deposition [107], we propose that *in vivo* treatment with 12 A12 mAb negatively interferes into hippocampus of 6-month-old Tg2576 mice with gradual mechanism of A β aggregation, as demonstrated by the reduction of the most toxic A11-positive, oligomeric conformers of A β (along with a reciprocal increase of monomeric form) we found in older animals. In support of the non-linear relationship existing *in vivo* between A β load and plaque formation, acute antibody-mediated targeting of pre-amyloid seeds in 3-month-old APP23 mice (during the sigmoidal lag phase of amyloid aggregation) is effective for prevention of cerebral amyloidosis and associated pathology up to 6 months, in spite of the precocious interruption of the treatment [108]. Experimental evidence in cellular and animal models

(See figure on next page.)

Fig. 9 Synaptic instability is relieved in aged Tg2576 mice following discontinuous immunization with 12 A12 mAb. **A,C,E,G,I** Representative images of Western blotting analysis ($n = 8$ animals per each group, 4 males and 4 females for each experimental condition) carried out on whole protein lysates of hippocampi from animals of three experimental groups (littermate wild-type, vehicle-treated Tg2576, Tg2576 + mAb) with antibodies for PSD95, synaptophysin, syntaxin SNAP25 and α -synuclein (as indicated alongside the blots). Arrows on the right side indicate the molecular weight (kDa) of bands calculated from migration of standard proteins. **B,D,F,H,J** Histograms show the semi-quantitative densitometry of the intensity signals of bands by normalization with β -actin level used as loading control. $p < 0.05$ is accepted as statistically significant (one-way ANOVA followed by Bonferroni's post-hoc test for multiple comparisons among more than two groups * $p < 0.05$; ** $p < 0.01$; *** $p < 0.0005$; **** $p < 0.0001$)

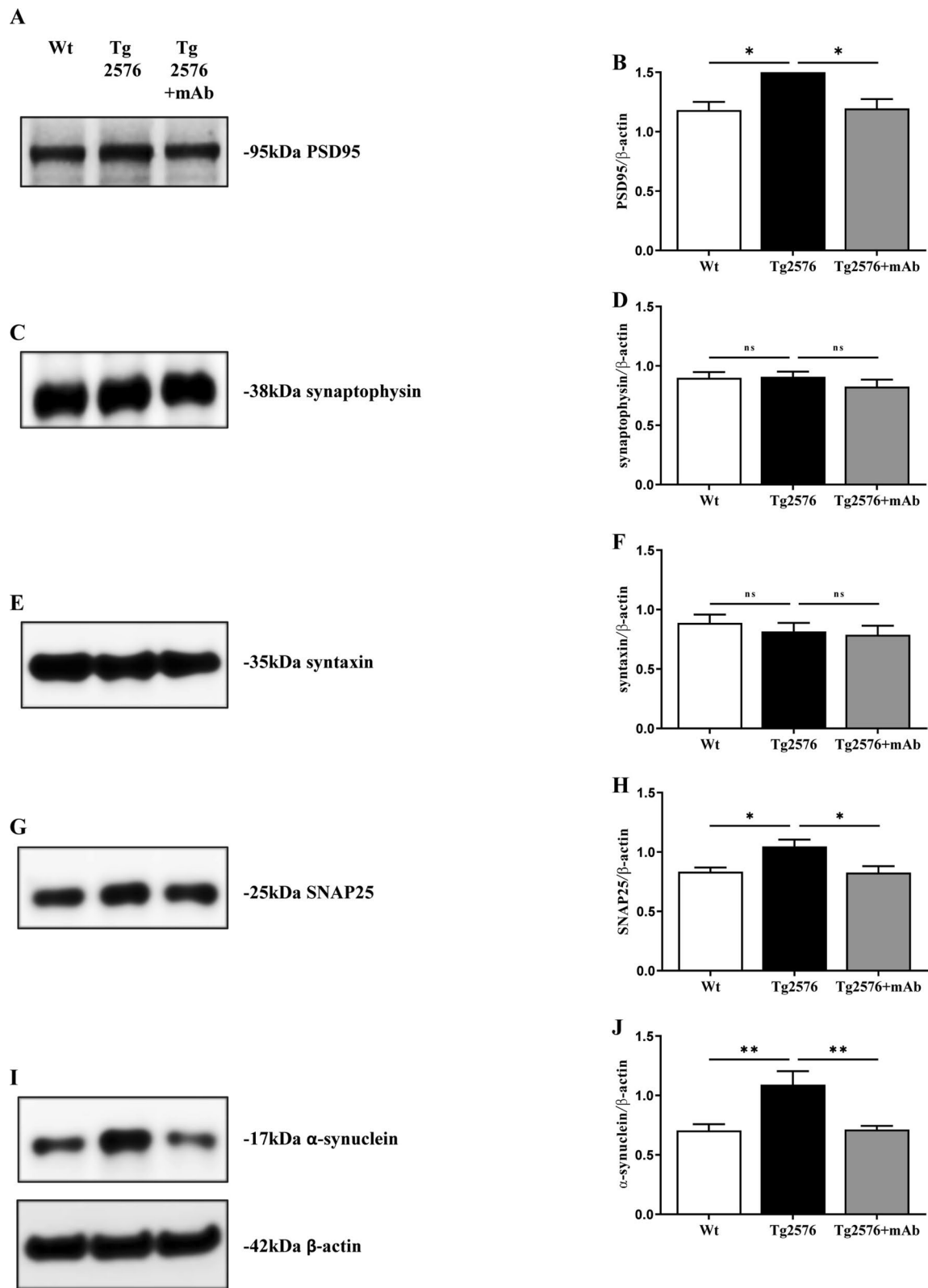


Fig. 9 (See legend on previous page.)

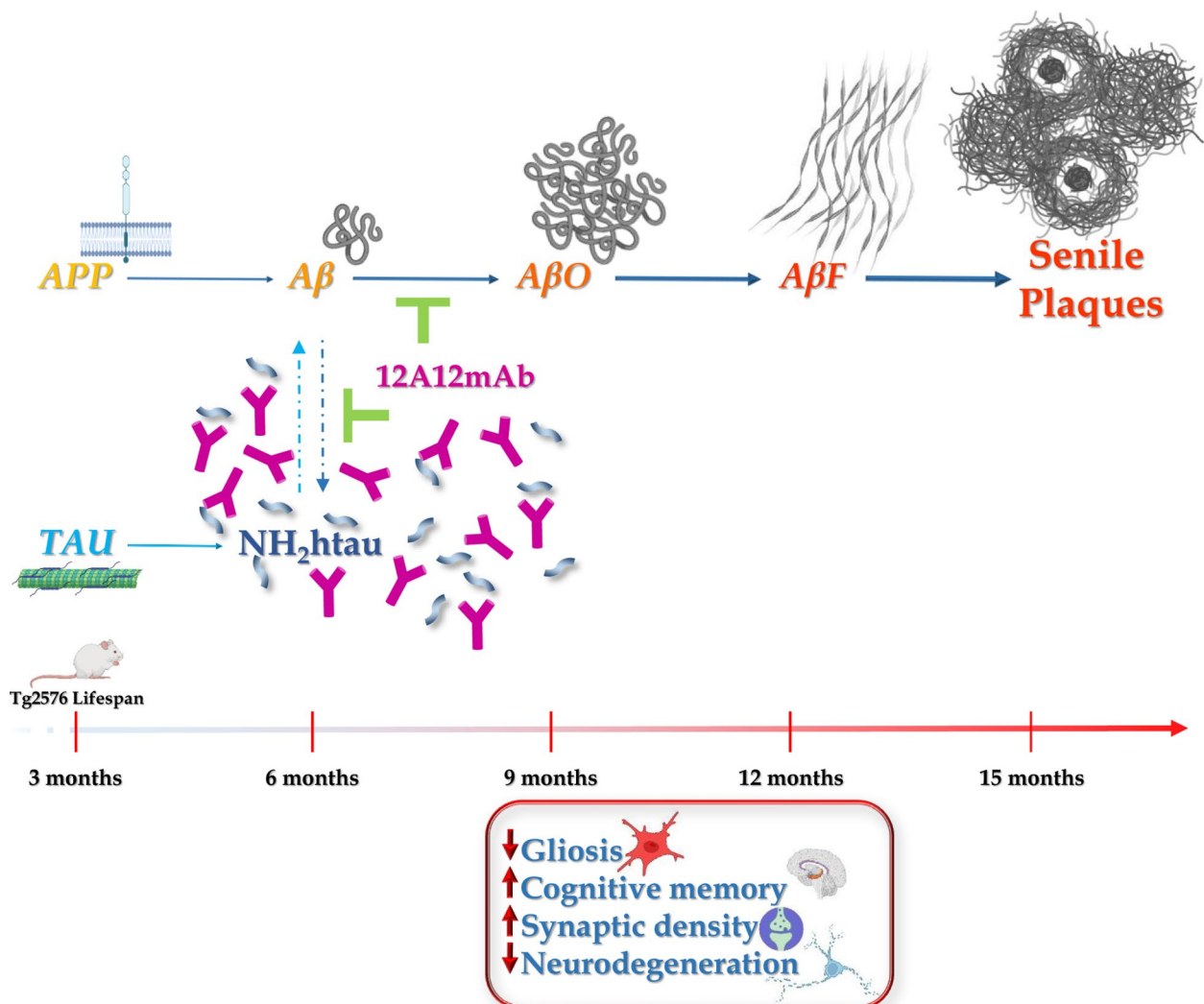


Fig. 10 Proposed mechanism(s) underlying the effect of 12 A12 mAb on toxic interplay between A β and Tau truncation during the pathobiology of AD. According to the the “Amyloid Hypothesis”, the abnormal amyloidogenic processing of Amyloid Precursor Protein (APP) triggers the accumulation of Amyloid beta (A β) that, in turn, causes downstream several post-translational modifications of Tau protein, including truncation with generation of the 20–22 kDa neurotoxic, N-terminal tau fragment(s) (NH₂htau) that is targeted by 12 A12 mAb [1]. During the gradual development of AD, the time-dependence aggregation A β takes place into the brain leading to formation of prefibrillar oligomeric intermediates (A β O), mature fibrils (A β F) and, eventually, senile plaques. Treatment with 12 A12 mAb in 6 month old Tg2576 APP/A β mouse model impacts not only on tau but also on APP/A β pathology [2, 21, 22] exerting (up to three months later) a beneficial action on gliosis, cognitive impairment, synaptic damage and neurodegeneration

have also shown that the toxicity of A β is directly linked to its aggregation state [84, 109] with the greatest clinical efficacy for antibodies reducing the cerebral A β amyloidosis [110]. In particular, during the temporal progression of AD, the 4kDa A β monomer slowly accumulates to a critical limit and, then, undergoes sequential changes in conformation and misfolding that cause its much faster assembly from transient and structurally heterogeneous intermediates, the so-called small oligomers and protofibrils, to mature high-molecular-weight insoluble fibrils

[111–116]. While the oligomers are synaptotoxic and can induce tau hyperphosphorylation and cleavage [117], the fibrillar senile plaques elicit proinflammatory responses, contributing to oxidative stress, neuronal degeneration and neuroinflammation [118]. Relevantly our data, by showing that the prolonged protective effect of 12 A12 mAb involves a net increase of the total amount of unaggregated A β without changing the expression level of APP and its amyloidogenic processing, are more in agreement with recent preclinical and clinical evidence

suggesting that AD may be to a certain extent due to a loss of function of the physiological levels of soluble A β monomer [119–123], in particular the longer and more-aggregation prone A β 1–42, which per se possesses several biological functions, including regulation of synaptic function, glucose metabolism and memory formation [124–128]. Nevertheless, whether the acute immunoneutralization of the NH₂tau with 12 A12 mAb can delay or even prevent much later in life the manifestation of the full-blown, dense ThS-positive amyloid plaque deposits becoming clearly detectable during lifespan of Tg2576 mice from 12–15-months of age onwards [27, 28, 60] is still under investigation. Likewise, whether the anti-amyloidogenic effect of this antibody targeting the N-terminal of tau is restricted to a precise and limited temporal window during which antibody-mediated antagonizing activity is most efficient in limiting the AD progression requires to be better investigated. Finally, whether the molecular mechanisms of neuroprotection involves direct and/or indirect interactions of antibody with protein(s) and its aggregates still needs to be clarified.

From a translational point of view, it is of particular relevance that the peripheral administration of 4 doses of 12 A12 mAb *in vivo* provides durable neuroprotection in the absence of any compound-related brain microhemorrhage, deleterious microgliosis or other pathologies. Two common side-effects of immunotherapy in aged APP-overexpressing preclinical mouse models are the excessive inflammatory response and the risk of vascular weakening and leakage in pial arteries, penetrating arteries and arterioles [129–133] that may be associated with capillary instability caused by antibody-induced redistribution of target species, in particular A β , in blood vessels or brain parenchyma [134, 135]. Early/middle symptomatic patients suffering from AD are assumed to require long-term and continuous administration of treatments throughout the life to prevent/hinder the cumulative build-up into their brain of both A β and tau pathologies and related cognitive decline with consequent potential side effects, including hemorrhagic risk and encephalitis future clinical applications, due to repeated injections and/or high cost of multiple infusions [128, 136–138]. Therefore, the optimization of the administration regimen is of paramount importance in the pipeline of “candidate” therapeutic antibodies in order to achieve higher clinical benefit, tolerability and safety with consequent amelioration in compliance of affected patients [137–139]. In this framework, our findings prospect that the temporary, not-invasive administration of 12 A12 mAb could be an effective intervention with low/moderate risk/benefit ratio for clinical management of AD, in the absence of unwanted secondary responses (vascular

congestion and glial cell activation) that may compromise its long-term therapeutic benefits.

Another important aspect is the apparent discrepancy that arises between the prolonged (up to three months) duration of therapeutic improvement detected in this strain on brain pathologies/cognition and the premature interruption in delivery of brain-penetrating 12 A12 mAb. This counterintuitive observation cannot be fully explained either by low penetrance and/or poor retention of 12 A12 mAb into their hippocampi (Suppl. Figure 1B–D) and by the half-life of mouse IgG ranging around 1 week in plasma [140–143]. To this point, we favour the hypothesis that the greatest efficacy of “candidate” therapeutic antibody depends on the ability of intercepting/engaging the co-pathogenetic link existing between A β and tau, especially in the preclinical phase of AD [144]. A dynamic and mutual interplay, rather than overall amount at a certain point in time, of abnormal soluble species of both A β and tau that accumulate and reciprocally influence over the years seems to be more closely associated with neuronal dysfunction in aging Tg2576 mice and in a way that is responsive to treatment with 12 A12 mAb. Consistent with the interpretation, acute (only for 5 days) and specific targeting of pre-fibrillar A β seeds by intraperitoneal injection of Aducanumab offers prolonged neuroprotection (up to 6 months) in APP23 mice by reducing not only the cerebral amount of congophilic plaque but also p-tau (AT8)-positive neuritic dystrophy [108]. A persistent therapeutic effect (up to 3 months after the last immunization) is detected following discontinuous (6 doses) intravenous injection of 43D (6–18aa) and 77E9 (184–195aa) antibodies targeting the N-terminal domain of tau in 3X Tg AD mice in concomitance with a reduction of APP and A β production [105]. Besides, a direct/local [145–150] and/or long-range [65, 151] interaction between specific types of misfolded tau (or its fragments) and A β (cross-seeding, aggregation and spreading) have been also described, further supporting the finding that tau is intertwined with amyloid maturation during the development of AD. Accordingly, we reported that the N-terminal half of tau binds and co-localizes with A β species into hippocampus of AD subjects [33, 152]. In addition, experiments of ThT fluorescence and turbidimetric measurements have shown that the extreme N-terminal tau fragment, including the 26–44 aminoacidic sequence that is specifically targeted by 12 A12 mAb [34], strongly accelerates the A β 1–42 aggregation *in vitro* with diminution in amorphous assemblies and parallel generation of highly-ordered amyloid fibrils [153, 154], in line with the *in vivo* action of 12 A12 mAb in inhibiting the A β rate of aggregation and, then, its proteotoxicity.

This study is not without limitations. First, although mouse and human tau aminoacidic sequences are different in the N-terminal region (residues 17 to 28 of human tau are not present in mouse) [155], 6 amino acid residues (Y29,T30,Q33,D34,Q35,E36) are present both in murine and primate tau sequence, as we previously discussed in another paper comparing side-by-side the *in vivo* effects of 12 A12 mAb targeting the 20–22kDa N-terminal tau fragments (NH₂htau) in both APP-overexpressing Tg2576 and 3xTg (APP Swedish, MAPT P301L, and PSEN1 M146 V) mice [2]. Besides, even though tau is an intrinsically disordered protein, its N-terminal domain (1–50 residues) displays several dynamic and local secondary structure elements such as isolated β -bridges, α -helices and 3-helix [156, 157]. In line with this statement, candidate tau antibodies tested for their therapeutic efficacy in clinical trials, including those recognizing post-translational modifications of protein, bind to epitopes usually ranging from 1–3 to 8–10 aminoacids that can be contiguous or not [158]. Experiments of alanine scanning mutagenesis and structural analyses of antibody-antigen complexes, aiming at clarifying whether the minimal sequence (antigenic determinants) required for recognition by the 12 A12 mAb involves a linear or conformational/discontinuous stretch of aminoacids, are currently under way. Second, interpretation of the reactivity of antibodies targeting the linear sequence of A β is not straightforward because of different sequence lengths and aggregation states of this 4kDa peptide and its proteolytic precursor (i.e. 12–14kDa β -secretase-derived APP fragment C99 or β CTF) with different biochemical and biophysical behaviours [159]. Therefore, different specificities and reactivities towards all the AD-relevant fragments generated by the APP proteolytic system (4kDa A β and its 12kDa trimers versus 12–14kDa β -secretase-derived APP fragment C99 or β CTF) might account for differences in intensity of immunoreactivity profile among multiple APP/A β antibodies used in our assays. To overcome these limitations, the use of multiple APP/A β antibodies and methodologies (Western blotting, immunofluorescence and dot-blot) have been selected within this experimental design.

Conclusions

Taken together, these findings highlight a therapeutically-targeted crosstalk occurring between tau and A β *in vivo*, opening up to future humanization of 12 A12 mAb for clinical treatment and mitigation of AD progression in humans.

Abbreviations

AD	Alzheimer's disease
NH ₂ htau	N-terminal tau fragment(s)
A β	Amyloid beta

APP	Amyloid precursor protein
mAb	Monoclonal antibody
H&E	Hematoxylin and eosin
ELISA	Enzyme-linked immunosorbent assay
WB	Western blotting
BACE1	Beta-secretase 1
GFAP	Glial fibrillary acidic protein
Iba1	Ionized calcium-binding adaptor molecule 1
α -syn	α -Synuclein
SNAP25	Synaptosomal-associated protein 25 kDa
PSD95	Postsynaptic density protein 95
GAPDH	Glyceraldehyde-3-Phosphate DeHydrogenase
NOR	Novel object recognition

Supplementary Information

The online version contains supplementary material available at <https://doi.org/10.1186/s40478-025-02022-y>.

Additional file 1
Additional file 2
Additional file 3
Additional file 4
Additional file 5

Acknowledgements

Not applicable

Author contributions

V.L. performed mice immunization and tissue dissection, Western Blotting, immunofluorescence and histological analyses, statistical analysis, data processing and interpretation of the results; M. De I. and A.P. performed behavioural test and analyzed data; F.M. and R.F. produced, purified the antibody 12 A12 mAb and validated its batch-to-batch consistency; B.O.B. performed microscopic analyses; G.Di N.; M.F.M.S., G.P., A.M. were involved in the project design, data analysis and interpretation of the results; provided funding; G.A. and P.C. designed and conceived study, carried out data processing and interpretation of the results, supervised all the experiments, wrote the manuscript, provided funding. All the authors read and approved the manuscript.

Funding

This research was funded by Alzheimer's Association Research Grant—Proposal ID: 971925 and Italian Ministry of Health (RF-2021–12374301). This work was also supported (in part) by Fondo Ordinario Enti (FOE D.M.865/2019) funds in the framework of a collaboration agreement between the Italian National Research Council and EBRI. Bijorn Omar Balzamino and Alessandra Micera are grateful to Italian Ministry of Health (RC278859) and Fondazione Roma (Rome, Italy).

Data availability

No datasets were generated or analysed during the current study.

Declarations

Ethics approval and consent to participate

All animal experiments were complied with the ARRIVE guidelines and were carried out in accordance with the ethical guidelines, the European Council Directive (2010/63/EU) and the Italian Animal Welfare legislation (D.L. 26/2014). The experimental approval was obtained from the Italian Ministry of Health (Authorization n. 1038–2020-PR; Authorization n. 419/2023-PR). This study was carried out according to the principles of the 3Rs (Replacement, Reduction and Refinement) to minimize animal suffering and to reduce the number of animals used.

Consent for publication

All authors have approved the manuscript and agree with its submission.

Competing interests

The authors declare there are no competing interests.

Author details

¹Institute of Translational Pharmacology (IFT)-National Research Council (CNR), Via Fosso del Cavaliere 100, 00133 Rome, Italy. ²European Brain Research Institute (EBRI), Viale Regina Elena 295, 00161 Rome, Italy. ³Centro Di Ricerca Europeo Sul Cervello (CERC), IRCCS Santa Lucia Foundation (FSL), Via Fosso del Fiorano 43-44, 00143 Rome, Italy. ⁴Department of Systems Medicine, University of Tor Vergata, Via Montpellier, 1, 00133 Rome, Italy. ⁵Institute of Nanotechnology Campus Ecotekne- National Research Council (CNR), Via Monteroni, 73100 Lecce, Italy. ⁶Research and Development Laboratory for Biochemical, Molecular and Cellular Applications in Ophthalmological Science, IRCCS-Fondazione Bietti, Via Santo Stefano Rotondo, 6, 00184 Rome, Italy. ⁷Institute of Crystallography (IC)-National Research Council (CNR), Via Paolo Gaifami 18, 95126 Catania, Italy.

Received: 13 March 2025 Accepted: 30 April 2025

Published online: 29 May 2025

References

- Amadoro G, Latina V, Calissano P (2021) A long story for a short peptide: therapeutic efficacy of a cleavage-specific tau antibody. *Neural Regen Res* 16(12):2417–2419. <https://doi.org/10.4103/1673-5374.313043>
- Corsetti V, Borreca A, Latina V, Giacobazzo G, Pignataro A, Krashia P, Natale F, Cocco S, Rinaudo M, Malerba F, Florio R, Ciarapica R, Coccurello R, D'Amelio M, Ammassari-Teule M, Grassi C, Calissano P, Amadoro G (2020) Passive immunotherapy for N-truncated tau ameliorates the cognitive deficits in two mouse Alzheimer's disease models. *Brain Commun* 2(1):039. <https://doi.org/10.1093/braincomms/fcaa039>
- Boxer AL, Sperling R (2023) Accelerating Alzheimer's therapeutic development: the past and future of clinical trials. *Cell* 186(22):4757–4772. <https://doi.org/10.1016/j.cell.2023.09.023>
- Cummings JL, Osse AML, Kinney JW, Cammann D, Chen J (2024) Alzheimer's disease: combination therapies and clinical trials for combination therapy development. *CNS Drugs* 38(8):613–624. <https://doi.org/10.1007/s40263-024-01103-1>
- Scheltens P, De Strooper B, Kivipelto M, Holstege H, Chételat G, Teunissen CE, Cummings J, van der Flier WM (2021) Alzheimer's disease. *Lancet* 397(10284):1577–1590. [https://doi.org/10.1016/S0140-6736\(20\)32205-4](https://doi.org/10.1016/S0140-6736(20)32205-4)
- DeTure MA, Dickson DW (2019) The neuropathological diagnosis of Alzheimer's disease. *Mol Neurodegener* 14(1):32. <https://doi.org/10.1186/s13024-019-0333-5>
- Ittner LM, Götz J (2011) Amyloid- β and tau—a toxic pas de deux in Alzheimer's disease. *Nat Rev Neurosci* 12(2):65–72. <https://doi.org/10.1038/nrn2967>
- Nisbet RM, Polanco JC, Ittner LM, Götz J (2015) Tau aggregation and its interplay with amyloid-beta. *Acta Neuropathol* 129(2):207–220. <https://doi.org/10.1007/s00401-014-1371-2>
- Rhein V, Song X, Wiesner A, Ittner LM, Baysang G, Meier F, Ozmen L, Bluethmann H, Dröse S, Brandt U, Savaskan E, Czech C, Götz J, Eckert A (2009) Amyloid-beta and tau synergistically impair the oxidative phosphorylation system in triple transgenic Alzheimer's disease mice. *Proc Natl Acad Sci U S A* 106(47):20057–20062. <https://doi.org/10.1073/pnas.0905529106>
- Pascoal TA, Mathotaarachchi S, Mohades S, Benedet AL, Chung C-O, Shin M, Wang S, Beaudry T, Kang MS, Soucy J-P, Labbe A, Gauthier S, Rosa-Neto P (2017) Amyloid- β and hyperphosphorylated tau synergy drives metabolic decline in preclinical Alzheimer's disease. *Mol Psychiatry* 22(2):306–311. <https://doi.org/10.1038/mp.2016.37>
- Desikan RS, McEvoy LK, Thompson WK, Holland D, Roddey JC, Blennow K, Aisen PS, Brewer JB, Hyman BT, Dale AM, Alzheimer's Disease Neuroimaging Initiative (2011) Amyloid- β associated volume loss occurs only in the presence of phospho-tau. *Ann Neurol* 70(4):657–661. <https://doi.org/10.1002/ana.22509>
- Fortea J, Vilaplana E, Alcolea D, Carmona-Iragui M, Sánchez-Saunders MB, Sala I, Antón-Aguirre S, González S, Medrano S, Pegueroles J, Morenas E, Clarimón J, Blesa R, Lleó A, Initiative ADN (2014) Cerebrospinal fluid β -amyloid and phospho-tau biomarker interactions affecting brain structure in preclinical Alzheimer disease. *Ann Neurol* 76(2):223–230. <https://doi.org/10.1002/ana.24186>
- Timmers M, Tesseur I, Bogert J, Zetterberg H, Blennow K, Börjesson-Hanson A, Baquero M, Boada M, Randolph C, Tritsmans L, Nueten LV, Engelborghs S, Streffer JR (2019) Relevance of the interplay between amyloid and tau for cognitive impairment in early Alzheimer's disease. *Neurobiol Aging* 79:131–141
- Roda AR, Serra-Mir G, Montoliu-Gaya L, Tiessler L, Villegas S (2022) Amyloid-beta peptide and tau protein crosstalk in Alzheimer's disease. *Neural Regen Res* 17(8):1666–1674. <https://doi.org/10.4103/1673-5374.332127>
- Salloway SP, Sevingy J, Budur K, Torleif Pederson J, DeMattos RB, Von Rosenstiel P, Paez A, Evans R, Weber CJ, Hendrix JA, Worley S, Bain LJ, Carrillo MC (2020) Advancing combination therapy for Alzheimer's disease. *Alzheimer's Dementia Transl Res Clin Interv* 6(1):e12073. <https://doi.org/10.1002/trc2.12073>
- Busche MA, Hyman BT (2020) Synergy between amyloid- β and tau in Alzheimer's disease. *Nat Neurosci* 23(10):1183–1193. <https://doi.org/10.1038/s41593-020-0687-6>
- Castellani RJ, Plascencia-Villa G, Perry G (2019) The amyloid cascade and Alzheimer's disease therapeutics: theory versus observation. *Lab Invest* 99(7):958–970. <https://doi.org/10.1038/s41374-019-0231-z>
- Koller EJ, Ibanez KR, Vo Q, McFarland KN, De La Cruz EG, Zobel L, Williams T, Xu G, Ryu D, Patel P, Giasson BI, Prokop S, Chakrabarty P (2022) Combinatorial model of amyloid β and tau reveals synergy between amyloid deposits and tangle formation. *Neuropathol Appl Neurobiol* 48(2):e12779. <https://doi.org/10.1111/nan.12779>
- Amadoro G, Latina V, Corsetti V (1866) Calissano P (2020) N-terminal tau truncation in the pathogenesis of Alzheimer's disease (AD): developing a novel diagnostic and therapeutic approach. *Biochim Biophys Acta Mol Basis Dis* 3:165584. <https://doi.org/10.1016/j.bbadis.2019.165584>
- Latina V, Giacobazzo G, Calissano P, Atlante A, La Regina F, Malerba F, Dell'Aquila M, Stigliano E, Balzamino BO, Micera A, Coccurello R, Amadoro G (2021) Tau cleavage contributes to cognitive dysfunction in strepto-zotocin-induced sporadic Alzheimer's disease (sAD) mouse model. *Int J Mol Sci* 22(22):12158. <https://doi.org/10.3390/ijms222212158>
- Latina V, De Introna M, Caligiuri C, Loviglio A, Florio R, La Regina F, Pignataro A, Ammassari-Teule M, Calissano P, Amadoro G (2023) Immunotherapy with cleavage-specific 12A12mAb reduces the tau cleavage in visual cortex and improves visuo-spatial recognition memory in Tg2576 AD mouse model. *Pharmaceutics* 15(2):509. <https://doi.org/10.3390/pharmaceutics15020509>
- Latina V, Atlante A, Malerba F, La Regina F, Balzamino BO, Micera A, Pignataro A, Stigliano E, Cavallaro S, Calissano P, Amadoro G (2023) The cleavage-specific Tau 12A12mAb exerts an anti-amyloidogenic action by modulating the endocytic and bioenergetic pathways in Alzheimer's disease mouse model. *Int J Mol Sci* 24(11):9683. <https://doi.org/10.3390/ijms24119683>
- Morello G, Guarnaccia M, La Cognata V, Latina V, Calissano P, Amadoro G, Cavallaro S (2023) Transcriptomic analysis in the hippocampus and retina of Tg2576 AD mice reveals defective mitochondrial oxidative phosphorylation and recovery by Tau 12A12mAb treatment. *Cells* 12(18):2254. <https://doi.org/10.3390/cells12182254>
- Hsiao K, Chapman P, Nilsen S, Eckman C, Harigaya Y, Younkin S, Yang F, Cole G (1996) Correlative memory deficits, A β elevation, and amyloid plaques in transgenic mice. *Science* 274(5284):99–102. <https://doi.org/10.1126/science.274.5284.99>
- Morales-Corraliza J, Mazzella MJ, Berger JD, Diaz NS, Choi JHK, Levy E, Matsuoka Y, Planell E, Mathews PM (2009) In vivo turnover of Tau and APP metabolites in the brains of wild-type and Tg2576 mice: greater stability of sAPP in the β -amyloid depositing mice. *PLoS ONE* 4(9):e7134. <https://doi.org/10.1371/journal.pone.0007134>
- Kawarabayashi T, Younkin LH, Saido TC, Shoji M, Ashe KH, Younkin SG (2001) Age-dependent changes in brain, CSF, and plasma amyloid (beta) protein in the Tg2576 transgenic mouse model of Alzheimer's disease. *J Neurosci* 21(2):372–381. <https://doi.org/10.1523/JNEUROSCI.21-02-00372.2001>
- Irizarry MC, McNamara M, Fedorchak K, Hsiao K, Hyman BT (1997) APPSw transgenic mice develop age-related A β deposits and

- neuropil abnormalities, but no neuronal loss in CA1. *J Neuropathol Exp Neurol* 56(9):965–973. <https://doi.org/10.1097/00005072-199709000-00002>
28. Noda-Saita K, Terai K, Iwai A, Tsukamoto M, Shitaka Y, Kawabata S, Okada M, Yamaguchi T, (2004) Exclusive association and simultaneous appearance of congophilic plaques and AT8-positive dystrophic neurites in Tg2576 mice suggest a mechanism of senile plaque formation and progression of neuritic dystrophy in Alzheimer's disease. *Acta Neuropathol* 108(5):435–442. <https://doi.org/10.1007/s00401-004-0907-2>
 29. Boyarko B, Hook V (2021) Human tau isoforms and proteolysis for production of toxic tau fragments in neurodegeneration. *Front Neurosci* 15:702788. <https://doi.org/10.3389/fnins.2021.702788>
 30. Quinn JP, Corbett NJ, Kellett KAB, Hooper NM (2018) Tau proteolysis in the pathogenesis of tauopathies: neurotoxic fragments and novel biomarkers. *J Alzheimers Dis* 63(1):13–33. <https://doi.org/10.3233/JAD-170959>
 31. Chu D, Yang X, Wang J, Zhou Y, Gu JH, Miao J, Wu F, Liu F (2024) Tau truncation in the pathogenesis of Alzheimer's disease: a narrative review. *Neural Regen Res*. 19(6):1221–32
 32. Sasaguri H, Nilsson P, Hashimoto S, Nagata K, Saito T, De Strooper B, Hardy J, Vassar R, Winblad B, Saido TC (2017) APP mouse models for Alzheimer's disease preclinical studies. *EMBO J* 36(17):2473–2487. <https://doi.org/10.15252/embj.201797397>
 33. Amadoro G, Corsetti V, Atlante A, Florenzano F, Capsoni S, Bussani R, Mercanti D, Calissano P (2012) Interaction between NH(2)-tau fragment and Aβ in Alzheimer's disease mitochondria contributes to the synaptic deterioration. *Neurobiol Aging* 33(4):833.e1–25. <https://doi.org/10.1016/j.neurobiolaging.2011.08.001>
 34. Florenzano F, Corsetti V, Ciasca G, Ciotti MT, Pittaluga A, Olivero G, Feligioni M, Iannuzzi F, Latina V, Sciacca MFM, Sinopoli A, Milardi D, Pappalardo G, De Spirito M, Papi M, Atlante A, Bobba A, Borreca A, Calissano P, Amadoro G (2017) Extracellular truncated tau causes early presynaptic dysfunction associated with Alzheimer's disease and other tauopathies. *Oncotarget* 8(39):64745–64778. <https://doi.org/10.18632/oncotarget.17371>
 35. Mort S, Buttle DJ (1999) The use of cleavage site specific antibodies to delineate protein processing and breakdown pathways. *Mol Pathol* 52(1):11–18. <https://doi.org/10.1136/mp.52.1.11>
 36. Rohn TT, Rissman RA, Davis MC, Kim YE, Cotman CW, Head E (2002) Caspase-9 activation and caspase cleavage of tau in the Alzheimer's disease brain. *Neurobiol Dis* 11(2):341–354. <https://doi.org/10.1006/nbdi.2002.0549>
 37. Corsetti V, Amadoro G, Gentile A, Capsoni S, Ciotti MT, Cencioni MT, Atlante A, Canu N, Rohn TT, Cattaneo A, Calissano P (2008) Identification of a caspase-derived N-terminal tau fragment in cellular and animal Alzheimer's disease models. *Mol Cell Neurosci* 38(3):381–392. <https://doi.org/10.1016/j.mcn.2008.03.011>
 38. Zhang D, Zhang W, Ming C, Gao X, Yuan H, Lin X, Mao X, Wang C, Guo X, Du Y, Shao L, Yang R, Lin Z, Wu X, Huang TY, Wang Z, Zhang YW, Xu H, Zhao Y (2024) P-tau217 correlates with neurodegeneration in Alzheimer's disease, and targeting p-tau217 with immunotherapy ameliorates murine tauopathy. *Neuron* 112(10):1676–1693.e12. <https://doi.org/10.1016/j.neuron.2024.02.017>
 39. Martín-Ávila A, Modak SR, Rajamohamedsait HB, Dodge A, Shamir DB, Krishnaswamy S, Sandusky-Beltran LA, Walker M, Lin J, Congdon EE, Sigurdsson EM (2024) Clearing truncated tau protein restores neuronal function and prevents microglia activation in tauopathy mice. *Biorxiv*. <https://doi.org/10.1101/2024.05.21.595198>
 40. Mably AJ, Kanmert D, Mc Donald JM, Liu W, Caldarone BJ, Lemere CA, O'Nuallain B, Kosik KS, Walsh DM (2015) Tau immunization: a cautionary tale? *Neurobiol Aging* 36(3):1316–1332. <https://doi.org/10.1016/j.neurobiolaging.2014.11.022>
 41. Borreca A, Latina V, Corsetti V, Middei S, Piccinin S, Della Valle F, Bussani R, Ammassari-Teule M, Nisticò R, Calissano P, Amadoro G (2018) AD-related N-terminal truncated tau is sufficient to recapitulate in vivo the early perturbations of human neuropathology: implications for immunotherapy. *Mol Neurobiol* 55(10):8124–8153. <https://doi.org/10.1007/s12035-018-0974-3>
 42. Amadoro G, Serafino AL, Barbato C, Ciotti MT, Sacco A, Calissano P, Canu N (2004) Role of N-terminal tau domain integrity on the survival of cerebellar granule neurons. *Cell Death Differ* 11(2):217–230. <https://doi.org/10.1038/sj.cdd.4401314>
 43. Amadoro G, Ciotti MT, Costanzi M, Cestari V, Calissano P, Canu N (2006) NMDA receptor mediates tau-induced neurotoxicity by calpain and ERK/MAPK activation. *Proc Natl Acad Sci U S A* 103(8):2892–2897. <https://doi.org/10.1073/pnas.0511065103>
 44. Antunes M, Biala G (2012) The novel object recognition memory: neurobiology, test procedure, and its modifications. *Cogn Process* 13(2):93–110. <https://doi.org/10.1007/s10339-011-0430-z>
 45. Barker GR, Warburton EC (2008) Critical role of the cholinergic system for object-in-place associative recognition memory. *Learn Mem* 16(1):8–11. <https://doi.org/10.1101/lm.1121309>
 46. Ennaceur A (2010) One-trial object recognition in rats and mice: methodological and theoretical issues. *Behav Brain Res* 215(2):244–254. <https://doi.org/10.1016/j.bbr.2009.12.036>
 47. Schagger H, von Jagow G (1987) Tricine-sodium dodecyl sulfate-polyacrylamide gel electrophoresis for the separation of proteins in the range from 1 to 100 kDa. *Anal Biochem* 166(2):368–379. [https://doi.org/10.1016/0003-2697\(87\)90587-2](https://doi.org/10.1016/0003-2697(87)90587-2)
 48. Kaye R, Head E, Thompson JL, McIntire TM, Milton SC, Cotman CW, Glabe CG (2003) Common structure of soluble amyloid oligomers implies common mechanism of pathogenesis. *Science* 300(5618):486–489. <https://doi.org/10.1126/science.1079469>
 49. Kaye R, Head E, Sarsoza F, Saing T, Cotman CW, Necula M, Margol L, Wu J, Breydo L, Thompson JL, Rasool S, Gurlo T, Butler P, Glabe CG (2007) Fibril-specific, conformation dependent antibodies recognize a generic epitope common to amyloid fibrils and fibrillar oligomers that is absent in prefibrillar oligomers. *Mol Neurodegener* 2:18. <https://doi.org/10.1186/1750-1326-2-18>
 50. Lefterov I, Fitz NF, Cronican A, Lefterov P, Staufenbiel M, Koldamova R (2009) Memory deficits in APP23/Abca1+/- mice correlate with the level of Aβ oligomers. *ASN Neuro* 1(2):e00006. <https://doi.org/10.1042/AN20090015>
 51. Liu P, Paulson JB, Forster CL, Shapiro SL, Ashe KH, Zahs KR (2015) Characterization of a novel mouse model of Alzheimer's disease-amyloid pathology and unique β-amyloid oligomer profile. *PLoS ONE* 10(5):e0126317. <https://doi.org/10.1371/journal.pone.0126317>
 52. Liu P, Reed MN, Kotilinek LA, Grant MKO, Forster CL, Qiang W, Shapiro SL, Reichl JH, Chiang ACA, Jankowsky JL, Wilmot CM, Cleary JP, Zahs KR, Ashe KH (2015) Quaternary structure defines a large class of amyloid-β oligomers neutralized by sequestration. *Cell Rep* 11(11):1760–1771. <https://doi.org/10.1016/j.celrep.2015.05.021>
 53. Paxinos G, Franklin KBJ (2001) The mouse brain in stereotaxic coordinates, 2nd edn. Academic Press, New York, NY, USA
 54. Bevins RA, Besheer J (2006) Object recognition in rats and mice: a one-trial non-matching-to-sample learning task to study "recognition memory." *Nat Protoc* 1(3):1306–1311. <https://doi.org/10.1038/nprot.2006.205>
 55. Clark RE, Zola SM, Squire LR (2000) Impaired recognition memory in rats after damage to the hippocampus. *J Neurosci* 20(23):8853–8860. <https://doi.org/10.1523/JNEUROSCI.20-23-08853.2000>
 56. Stewart S, Cacucci F, Lever C (2011) Which memory task for my mouse? A systematic review of spatial memory performance in the Tg2576 Alzheimer's mouse model. *J Alzheimers Dis* 26(1):105–126. <https://doi.org/10.3233/JAD-2011-101827>
 57. Grayson B, Leger M, Piercy C, Adamson L, Harte M, Neill JC (2015) Assessment of disease-related cognitive impairments using the novel object recognition (NOR) task in rodents. *Behav Brain Res* 285:176–193. <https://doi.org/10.1016/j.bbr.2014.10.025>
 58. Dorostkar MM, Burgold S, Filser S, Barghorn S, Schmidt B, Anumala UR, Hillen H, Klein C, Herms J (2014) Immunotherapy alleviates amyloid-associated synaptic pathology in an Alzheimer's disease mouse model. *Brain* 137(Pt 12):3319–3326. <https://doi.org/10.1093/brain/awu280>
 59. Morales-Corraliza J, Schmidt SD, Mazzella MJ, Berger JD, Wilson DA, Wesson DW, Jucker M, Levy E, Nixon RA, Mathews PM (2013) Immunization targeting a minor plaque constituent clears β-amyloid and rescues behavioral deficits in an Alzheimer's disease mouse model. *Neurobiol Aging* 34(1):137–145. <https://doi.org/10.1016/j.neurobiolaging.2012.04.007>
 60. Castillo-Carranza DL, Guerrero-Muñoz MJ, Sengupta U, Hernandez C, Barrett ADT, Dineley K, Kaye R (2015) Tau immunotherapy modulates

- both pathological tau and upstream amyloid pathology in an Alzheimer's disease mouse model. *J Neurosci* 35(12):4857–4868. <https://doi.org/10.1523/JNEUROSCI.4989-14.2015>
61. Alvarez P, Zola-Morgan S, Squire LR (1995) Damage limited to the hippocampal region produces long-lasting memory impairment in monkeys. *J Neurosci* 15(5 Pt 2):3796–3807. <https://doi.org/10.1523/JNEUROSCI.15-05-03796.1995>
 62. Yonelinas A, Hawkins C, Abovian A, Aly M (2024) The role of recollection, familiarity, and the hippocampus in episodic and working memory. *Neuropsychologia* 193:108777. <https://doi.org/10.1016/j.neuropsychologia.2023.108777>
 63. Braak H, Braak E (1991) Neuropathological staging of Alzheimer-related changes. *Acta Neuropathol* 82(4):239–259. <https://doi.org/10.1007/BF00308809>
 64. Eisele YS, Duyckaerts C (2016) Propagation of A β pathology: hypotheses, discoveries, and yet unresolved questions from experimental and human brain studies. *Acta Neuropathol* 131(1):5–25. <https://doi.org/10.1007/s00401-015-1516-y>
 65. Lee WJ, Brown JA, Kim HR, La Joie R, Cho H, Lyoo CH, Rabinovici GD, Seong JK, Seeley WW (2022) Alzheimer's disease neuroimaging initiative regional A β -tau interactions promote onset and acceleration of Alzheimer's disease tau spreading. *Neuron* 110(12):1932–1943.e5. <https://doi.org/10.1016/j.neuron.2022.03.034>
 66. Wang ZT, Zhang C, Wang YJ, Dong Q, Tan L, Yu JT (2020) Selective neuronal vulnerability in Alzheimer's disease. *Ageing Res Rev* 62:101114. <https://doi.org/10.1016/j.arr.2020.101114>
 67. Kouznetsova E, Klingner M, Sorger D, Sabri O, Grossmann U, Steinbach J, Scheunemann M, Schliebs R (2006) Developmental and amyloid plaque-related changes in cerebral cortical capillaries in transgenic Tg2576 Alzheimer mice. *Int J Dev Neurosci* 24(2–3):187–193. <https://doi.org/10.1016/j.jdevneu.2005.11.011>
 68. Takano T, Han X, Deane R, Zlokovic B, Nedergaard M (2007) Two-photon imaging of astrocytic Ca $^{2+}$ signaling and the microvasculature in experimental mice models of Alzheimer's disease. *Ann N Y Acad Sci* 1097:40–50. <https://doi.org/10.1196/annals.1379.004>
 69. Wang K, Zhang B, Du H, Duan H, Jiang Z, Fang S (2024) Research landscape and trends of cerebral amyloid angiopathy: a 25-year scientometric analysis. *Front Neurol* 14:1334360. <https://doi.org/10.3389/fneur.2023.1334360>
 70. Spire-Jones TL, Attems J, Thal DR (2017) Interactions of pathological proteins in neurodegenerative diseases. *Acta Neuropathol* 134(2):187–205. <https://doi.org/10.1007/s00401-017-1709-7>
 71. Adlard PA, Cherny JP, Finkelstein DI, Gautier E, Robb E, Cortes M, Volitakis I, Liu X, Smith JP, Perez K, Loughton K, Li QX, Charman SA, Nicolazzo JA, Wilkins S, Delewa K, Lynch T, Kok G, Ritchie CW, Tanzi RE, Cappai R, Masters CL, Barnham KJ, Bush AI (2008) Rapid restoration of cognition in Alzheimer's transgenic mice with 8-hydroxy quinoline analogs is associated with decreased interstitial A β . *Neuron* 59(1):43–55. <https://doi.org/10.1016/j.neuron.2008.06.018>
 72. Afram E, Lauritzen I, Bourgeois A, El Mana W, Duplan E, Chami M, Valverde A, Charlotte B, Pardossi-Piquard R, Checler F (2023) The η -secretase-derived APP fragment η CTF is localized in Golgi, endosomes and extracellular vesicles and contributes to A β production. *Cell Mol Life Sci* 80(4):97. <https://doi.org/10.1007/s00018-023-04737-4>
 73. Westerman MA, Cooper-Blacketer D, Mariash A, Kotilinek L, Kawarabayashi T, Younkin LH, Carlson GA, Younkin SG, Ashe KH (2002) The relationship between A β and memory in the Tg2576 mouse model of Alzheimer's disease. *J Neurosci* 22(5):1858–1867. <https://doi.org/10.1523/JNEUROSCI.22-05-01858.2002>
 74. Takahashi RH, Capetillo-Zarate E, Lin MT, Milner TA, Gouras GK (2013) Accumulation of intraneuronal beta-amyloid 42 peptides is associated with early changes in microtubule-associated protein 2 in neurites and synapses. *PLoS ONE* 8(1):e51965. <https://doi.org/10.1371/journal.pone.0051965>
 75. Pignataro A, Meli G, Pagano R, Fontebasso V, Battistella R, Conforto G, Ammassari-Teule M, Middei S (2019) Activity-induced amyloid- β oligomers drive compensatory synaptic rearrangements in brain circuits controlling memory of presymptomatic Alzheimer's disease mice. *Biol Psychiatry* 86(3):185–195. <https://doi.org/10.1016/j.biopsych.2018.10.018>
 76. Musardo S, Therin S, Pelucchi S, D'Andrea L, Stringhi R, Ribeiro A, Manca A, Balducci C, Pagano J, Sala C, Verpelli C, Grieco V, Edefonti V, Forloni G, Gardoni F, Meli G, Di Marino D, Di Luca M, Marcello E (2022) The development of ADAM10 endocytosis inhibitors for the treatment of Alzheimer's disease. *Mol Ther* 30(7):2474–2490. <https://doi.org/10.1016/j.ymthe.2022.03.024>
 77. Kostylev MA, Kaufman AC, Nygaard HB, Patel P, Haas LT, Gunther EC, Vortmeyer A, Strittmatter SM (2015) Prion-protein-interacting amyloid- β oligomers of high molecular weight are tightly correlated with memory impairment in multiple Alzheimer mouse models. *J Biol Chem* 290(28):17415–17438. <https://doi.org/10.1074/jbc.M115.643577>
 78. Wu JW, Breydo L, Isas JM, Lee J, Kuznetsov YG, Lengen R, Glabe C (2010) Fibrillar oligomers nucleate the oligomerization of monomeric amyloid beta but do not seed fibril formation. *J Biol Chem* 285(9):6071–6079. <https://doi.org/10.1074/jbc.M109.069542>
 79. Sarsoza F, Saing T, Kaye R, Dahlin R, Dick M, Broadwater-Hollifield C, Mobley S, Lott I, Doran E, Gillen D, Anderson-Bergman C, Cribbs DH, Glabe C, Head E (2009) A fibril-specific, conformation-dependent antibody recognizes a subset of A β plaques in Alzheimer disease, Down syndrome and Tg2576 transgenic mouse brain. *Acta Neuropathol* 118(4):505–517. <https://doi.org/10.1007/s00401-009-0530-3>
 80. Maezawa I, Hong HS, Liu R, Wu CY, Cheng RH, Kung MP, Kung HF, Lam KS, Oddo S, Laferla FM, Jin LW (2008) Congo red and thioflavin-T analogs detect A β oligomers. *J Neurochem* 104(2):457–468. <https://doi.org/10.1111/j.1471-4159.2007.04972.x>
 81. Habashi M, Vutla S, Tripathi K, Senapati S, Chauhan PS, Haviv-Chesner A, Richman M, Mohand SA, Dumulon-Perreault V, Mulamreddy R, Okun E, Chill JH, Guérin B, Lubell WD, Rahimpour S (2022) Early diagnosis and treatment of Alzheimer's disease by targeting toxic soluble A β oligomers. *Proc Natl Acad Sci U S A* 119(49):e2210766119. <https://doi.org/10.1073/pnas.2210766119>
 82. Oakley H, Cole SL, Logan S, Maus E, Shao P, Craft J, Guillozet-Bongaarts A, Ohno M, Disterhoft J, Van Eldik L, Berry R, Vassar R (2006) Intraneuronal beta-amyloid aggregates, neurodegeneration, and neuron loss in transgenic mice with five familial Alzheimer's disease mutations: potential factors in amyloid plaque formation. *J Neurosci* 26(40):10129–10140. <https://doi.org/10.1523/JNEUROSCI.1202-06.2006>
 83. Pascoal TA, Benedet AL, Ashton NJ, Kang MS, Theriault J, Chamoun M, Savard M, Lussier FZ, Tissot C, Karikari TK, Ottoy J, Mathotaarachchi S, Stevenson J, Massarweh G, Schöll M, de Leon MJ, Soucy JP, Edison P, Blennow K, Zetterberg H, Gauthier S, Rosa-Neto P (2021) Microglial activation and tau propagate jointly across Braak stages. *Nat Med* 27(9):1592–1599. <https://doi.org/10.1038/s41591-021-01456-w>
 84. Long JM, Holtzman DM (2019) Alzheimer disease: an update on pathobiology and treatment strategies. *Cell* 179(2):312–339. <https://doi.org/10.1016/j.cell.2019.09.001>
 85. Meftah S, Gan J (2023) Alzheimer's disease as a synaptopathy: evidence for dysfunction of synapses during disease progression. *Front Synaptic Neurosci* 15:1129036. <https://doi.org/10.3389/fnsyn.2023.1129036>
 86. Kamphuis W, Mamber C, Moeton M, Kooijman L, Sluijs JA, Jansen AH, Verveer M, de Groot LR, Smith VD, Rangarajan S, Rodríguez JJ, Orre M, Hol EM (2012) GFAP isoforms in adult mouse brain with a focus on neurogenic astrocytes and reactive astrogliosis in mouse models of Alzheimer disease. *PLoS ONE* 7(8):e42823. <https://doi.org/10.1371/journal.pone.0042823>
 87. Lorenzini L, Giuliani A, Sivilia S, Baldassarro VA, Fernandez M, Lotti Margotti M, Giardino L, Fontani V, Rinaldi S, Calzà L (2016) REAC technology modifies pathological neuroinflammation and motor behaviour in an Alzheimer's disease mouse model. *Sci Rep* 6:35719. <https://doi.org/10.1038/srep35719>
 88. Ito D, Imai Y, Ohsawa K, Nakajima K, Fukuuchi Y, Kohsaka S (1998) Microglia-specific localisation of a novel calcium binding protein, Iba1. *Brain Res Mol Brain Res* 57(1):1–9. [https://doi.org/10.1016/s0169-328x\(98\)00040-0](https://doi.org/10.1016/s0169-328x(98)00040-0)
 89. Sasaki Y, Ohsawa K, Kanazawa H, Kohsaka S, Imai Y (2001) Iba1 is an actin-cross-linking protein in macrophages/microglia. *Biochem Biophys Res Commun* 286(2):292–297. <https://doi.org/10.1006/bbrc.2001.5388>
 90. Rajamohamedsait H, Rasool S, Rajamohamedsait W, Lin Y, Sigurdsson EM (2017) Prophylactic active tau immunization leads to sustained reduction in both tau and amyloid- β pathologies in 3xTg mice. *Sci Rep* 7(1):17034. <https://doi.org/10.1038/s41598-017-17313-1>

91. Wilcock DM, DiCarlo G, Henderson D, Jackson J, Clarke K, Ugen KE, Gordon MN, Morgan D (2003) Intracranially administered anti-A β antibodies reduce β -amyloid deposition by mechanisms both independent of and associated with microglial activation. *J Neurosci* 23(9):3745–3751. <https://doi.org/10.1523/JNEUROSCI.23-09-03745.2003>
92. Das P, Howard V, Loosbrock N, Dickson D, Murphy MP, Golde TE (2003) Amyloid-beta immunization effectively reduces amyloid deposition in FcRgamma-/- knock-out mice. *J Neurosci* 23(24):8532–8538. <https://doi.org/10.1523/JNEUROSCI.23-24-08532>
93. Das P, Smithson LA, Price RW, Holloway VM, Levites Y, Chakrabarty P, Golde TE (2006) Interleukin-1 receptor 1 knockout has no effect on amyloid deposition in Tg2576 mice and does not alter efficacy following A β immunotherapy. *J Neuroinflammation* 3:17. <https://doi.org/10.1186/1742-2094-3-17>
94. Matsuoka Y, Picciano M, Malester B, LaFrancois J, Zehr C, Daeschner JM, Olshchawka JA, Fonseca MI, O'Banion MK, Tenner AJ, Lemere CA, Duff K (2001) Inflammatory responses to amyloidosis in a transgenic mouse model of Alzheimer's disease. *Am J Pathol* 158(4):1345–1354. [https://doi.org/10.1016/S0002-9440\(10\)64085-0](https://doi.org/10.1016/S0002-9440(10)64085-0)
95. Jin P, Kim JA, Choi DY, Lee YJ, Jung HS, Hong JT (2013) Anti-inflammatory and anti-amyloidogenic effects of a small molecule, 2,4-bis(p-hydroxyphenyl)-2-butenol in Tg2576 Alzheimer's disease mice model. *J Neuroinflammation* 10:2. <https://doi.org/10.1186/1742-2094-10-2>
96. Radde R, Bolmont T, Kaeser SA, Coomaraswamy J, Lindau D, Stoltz L, Calhoun ME, Jäggi F, Wolburg H, Gengler S, Haass C, Ghetti B, Czech C, Hölscher C, Mathews PM, Jucker M (2006) A β 42-driven cerebral amyloidosis in transgenic mice reveals early and robust pathology. *EMBO Rep* 7(9):940–946. <https://doi.org/10.1038/sj.embor.7400784>
97. Fügner P, Hefendehl JK, Veeraghavalu K, Wendeln AC, Schlosser C, Obermüller U, Wegenast-Braun BM, Neher JJ, Martus P, Kohsaka S, Thunemann M, Feil R, Sisodia SS, Skodras A, Jucker M (2017) Microglia turnover with aging and in an Alzheimer's model via long-term in vivo single-cell imaging. *Nat Neurosci* 20(10):1371–1376. <https://doi.org/10.1038/nn.4631>
98. Kater MSJ, Huffels CFM, Oshima T, Renckens NS, Middeldorp J, Boddeke EWGM, Smit AB, Eggen BJL, Hol EM, Verheijen MHG (2023) Prevention of microgliosis halts early memory loss in a mouse model of Alzheimer's disease. *Brain Behav Immun* 107:225–241. <https://doi.org/10.1016/j.bbi.2022.10.009>
99. Dong H, Martin MV, Chambers S, Csernansky JG (2007) Spatial relationship between synapse loss and β -amyloid deposition in Tg2576 mice. *J Comp Neurol* 500(2):311–321. <https://doi.org/10.1002/cne.21176>
100. Kawarabayashi T, Shoji M, Younkin LH, Wen-Lang L, Dickson DW, Murakami T, Matsubara E, Abe K, Ashe KH, Younkin SG (2004) Dimeric amyloid beta protein rapidly accumulates in lipid rafts followed by apolipoprotein E and phosphorylated tau accumulation in the Tg2576 mouse model of Alzheimer's disease. *J Neurosci* 24(15):3801–3809. <https://doi.org/10.1523/JNEUROSCI.5543-03.2004>
101. Otth C, Concha II, Arendt T, Stieler J, Schliebs R, Gonzalez-Billault C, Maccioni RB (2002) A β 42 induces cdk5-dependent tau hyperphosphorylation in transgenic mice Tg2576. *J Alzheimers Dis* 4(5):417–430. <https://doi.org/10.3233/jad-2002-4508>
102. Tomidokoro K, Ishiguro Y, Harigaya E, Matsubara M, Ikeda JM, Park K, Yasutake T, Kawarabayashi K, Okamoto M, Shoji M (2001) A β 42 amyloidosis induces the initial stage of tau accumulation in APP(Sw) mice. *Neurosci Lett* 299(3):169–172. [https://doi.org/10.1016/S0304-3940\(00\)01767-5](https://doi.org/10.1016/S0304-3940(00)01767-5)
103. Plotkin SS, Cashman NR (2020) Passive immunotherapies targeting A β and tau in Alzheimer's disease. *Neurobiol Dis* 144:105010. <https://doi.org/10.1016/j.nbd.2020.105010>
104. Dai CL, Chen X, Kazim SF, Liu F, Gong CX, Grundke-Iqbal I, Iqbal K (2015) Passive immunization targeting the N-terminal projection domain of tau decreases tau pathology and improves cognition in a transgenic mouse model of Alzheimer disease and tauopathies. *J Neural Transm (Vienna)* 122(4):607–617. <https://doi.org/10.1007/s00702-014-1315-y>
105. Dai CL, Tung YC, Liu F, Gong CX, Iqbal K (2017) Tau passive immunization inhibits not only tau but also A β pathology. *Alzheimers Res Ther* 9(1):1. <https://doi.org/10.1186/s13195-016-0227-5>
106. Dai CL, Hu W, Tung YC, Liu F, Gong CX, Iqbal K (2018) Tau passive immunization blocks seeding and spread of Alzheimer hyperphosphorylated Tau-induced pathology in 3 \times Tg-AD mice. *Alzheimers Res Ther* 10(1):13. <https://doi.org/10.1186/s13195-018-0341-7>
107. Karlinski RA, Rosenthal A, Kobayashi D, Pons J, Alamed J, Mercer M, Li Q, Gordon MN, Gottschall PE, Morgan D (2009) Suppression of amyloid deposition leads to long-term reductions in Alzheimer's pathologies in Tg2576 mice. *J Neurosci* 29(15):4964–4971. <https://doi.org/10.1523/JNEUROSCI.4560-08.2009>
108. Uhlmann RE, Rother C, Rasmussen J, Schelle J, Bergmann C, Ullrich Gavilanes EM, Fritsch SK, Buehler A, Baumann F, Skodras A, Al-Shaana R, Beschoner N, Ye L, Kaeser SA, Obermüller U, Christensen S, Kartberg F, Stavenhagen JB, Rahfeld JU, Cynis H, Qian F, Weinreb PH, Bussiere T, Walker LC, Staufienbiel M, Jucker M (2020) Acute targeting of pre-amyloid seeds in transgenic mice reduces Alzheimer-like pathology later in life. *Nat Neurosci* 23(12):1580–1588. <https://doi.org/10.1038/s41593-020-00737-w>
109. Rother C, Uhlmann RE, Müller SA, Schelle J, Skodras A, Obermüller U, Häslér LM, Lambert M, Baumann F, Xu Y, Bergmann C, Salvadori G, Loos M, Brzak I, Shimshek D, Neumann U, Walker LC, Schultz SA, Chhatwal JP, Kaeser SA, Lichtenthaler SF, Staufienbiel M, Jucker M (2022) Experimental evidence for temporal uncoupling of brain A β deposition and neurodegenerative sequelae. *Nat Commun* 13(1):7333. <https://doi.org/10.1038/s41467-022-34538-5>
110. Vogt AS, Jennings GT, Mohsen MO, Vogel M, Bachmann MF (2023) Alzheimer's disease: a brief history of immunotherapies targeting amyloid β . *Int J Mol Sci* 24(4):3895. <https://doi.org/10.3390/ijms24043895>
111. Jagust WJ, Landau SM, Initiative ADN (2021) Temporal dynamics of β -amyloid accumulation in aging and Alzheimer disease. *Neurology* 96(9):e1347–e1357. <https://doi.org/10.1212/WNL.00000000000011524>
112. Hampel H, Hardy J, Blennow K, Chen C, Perry G, Kim SH, Villemagne VL, Aisen P, Vendruscolo M, Iwatsubo T, Masters CL, Cho M, Lannfelt L, Cummings JL, Vergallo A (2021) The amyloid- β pathway in Alzheimer's disease. *Mol Psychiatry* 26(10):5481–5503. <https://doi.org/10.1038/s41380-021-01249-0>
113. Glabe CG (2006) Common mechanisms of amyloid oligomer pathogenesis in degenerative disease. *Neurobiol Aging* 27(4):570–575. <https://doi.org/10.1016/j.neurobiolaging.2005.04.017>
114. Glabe CG (2008) Structural classification of toxic amyloid oligomers. *J Biol Chem* 283(44):29639–29643. <https://doi.org/10.1074/jbc.R800016200>
115. Ahmed M, Davis J, Aucoin D, Sato T, Ahuja S, Aimoto S, Elliott JI, Van Nostrand WE, Smith SO (2010) Structural conversion of neurotoxic amyloid-beta(1–42) oligomers to fibrils. *Nat Struct Mol Biol* 17(5):561–567. <https://doi.org/10.1038/nsmb.1799>
116. Sengupta U, Nilson AN, Kaye R (2016) The role of amyloid- β oligomers in toxicity, propagation, and immunotherapy. *EBioMedicine* 6:42–49. <https://doi.org/10.1016/j.ebiom.2016.03.035>
117. Viola KL, Klein WL (2015) Amyloid β oligomers in Alzheimer's disease pathogenesis, treatment, and diagnosis. *Acta Neuropathol* 129(2):183–206. <https://doi.org/10.1007/s00401-015-1386-3>
118. Pinheiro L, Faustino C (2019) Therapeutic strategies targeting amyloid- β in Alzheimer's disease. *Curr Alzheimer Res* 16(5):418–452. <https://doi.org/10.2174/1567205016666190321163438>
119. Giuffrida ML, Caraci F, Pignataro B, Cataldo S, De Bona P, Bruno V, Molinaro G, Pappalardo G, Messina A, Palmigiano A, Garozzo D, Nicoletti F, Rizzarelli E (2009) Copani A (2009) Beta-amyloid monomers are neuroprotective. *J Neurosci* 29(34):10582–10587. <https://doi.org/10.1523/JNEUROSCI.1736-09.2009>
120. Brothers HM, Gosztyla ML, Robinson SR (2018) The physiological roles of amyloid-beta peptide hint at new ways to treat Alzheimer's disease. *Front Aging Neurosci* 10:118. <https://doi.org/10.3389/fnagi.2018.00118>
121. Kent SA, Spire-Jones TL, Durrant CS (2020) The physiological roles of tau and A β : implications for Alzheimer's disease pathology and therapeutics. *Acta Neuropathol* 140(4):417–447. <https://doi.org/10.1007/s00401-020-02196-w>
122. Duan Y, Lv J, Zhang Z, Chen Z, Wu H, Chen J, Chen Z, Yang J, Wang D, Liu Y, Chen F, Tian Y, Cao X (2022) Exogenous A β 1–42 monomers improve synaptic and cognitive function in Alzheimer's disease model mice. *Neuropharmacology* 209:109002. <https://doi.org/10.1016/j.neuropharm.2022.109002>

123. Abanto J, Dwivedi AK, Imbimbo BP, Espay AJ (2024) Increases in amyloid- β 42 slow cognitive and clinical decline in Alzheimer's disease trials. *Brain* 147(10):3513–3521. <https://doi.org/10.1093/brain/awae216>
124. Puzzo D, Privitera L, Leznik E, Fa M, Staniszewski A, Palmeri A, Arancio O (2008) Picomolar amyloid-beta positively modulates synaptic plasticity and memory in hippocampus. *J Neurosci* 28(53):14537–14545. <https://doi.org/10.1523/JNEUROSCI.2692-08.2008>
125. Giuffrida ML, Tomasello MF, Pandini G, Caraci F, Battaglia G, Busceti C, Di Pietro P, Pappalardo G, Attanasio F, Chiechio S, Bagnoli S, Nacmias B, Sorbi S, Vigneri R, Rizzarelli E, Nicoletti F, Copani A (2015) Monomeric ss-amyloid interacts with type-1 insulin-like growth factor receptors to provide energy supply to neurons. *Front Cell Neurosci* 7(9):297. <https://doi.org/10.3389/fncel.2015.00297>
126. Fedele E (2023) Anti-amyloid therapies for alzheimer's disease and the amyloid cascade hypothesis. *Int J Mol Sci* 24(19):14499. <https://doi.org/10.3390/ijms241914499>
127. Cai W, Li L, Sang S, Pan X, Zhong C (2023) Physiological roles of β -amyloid in regulating synaptic function: implications for AD pathophysiology. *Neurosci Bull* 39(8):1289–1308. <https://doi.org/10.1007/s12264-022-00985-9>
128. Zhang Y, Chen H, Li R, Sterling K, Song W (2023) Amyloid β -based therapy for Alzheimer's disease: challenges, successes and future. *Signal Transduct Target Ther* 8(1):248. <https://doi.org/10.1038/s41392-023-01484-7>
129. Pfeifer M, Boncristiano S, Bondolfi L, Stalder A, Deller T, Staufenbiel M, Mathews PM, Jucker M (2002) Cerebral hemorrhage after passive anti-A β immunotherapy. *Science* 298(5597):1379. <https://doi.org/10.1126/science.1078259>
130. Racke MM, Boone LI, Hepburn DL, Parsadanian M, Bryan MT, Ness DK, Pirooz KS, Jordan WH, Brown DD, Hoffman WP, Holtzman DM, Bales KR, Gitter BD, May PC, Paul SM, DeMattos RB (2005) Exacerbation of cerebral amyloid angiopathy-associated microhemorrhage in amyloid precursor protein transgenic mice by immunotherapy is dependent on antibody recognition of deposited forms of amyloid beta. *J Neurosci* 25(3):629–636. <https://doi.org/10.1523/JNEUROSCI.4337-04.2005>
131. Zago W, Schroeter S, Guido T, Khan K, Seubert P, Yednock T, Schenk D, Gregg KM, Games D, Bard F, Kinney GG (2013) Vascular alterations in PDAPP mice after anti-A β immunotherapy: Implications for amyloid-related imaging abnormalities. *Alzheimers Dement* 9(5 Suppl):S105–S115. <https://doi.org/10.1016/j.jalz.2012.11.010>
132. Villarreal S, Zhao F, Hyde LA, Holder D, Forest T, Sondey M, Chen X, Sur C, Parker EM, Kennedy ME (2017) Chronic verubecestat treatment suppresses amyloid accumulation in advanced aged Tg2576-A β PPsw mice without inducing microhemorrhage. *J Alzheimers Dis* 59(4):1393–1413. <https://doi.org/10.3233/JAD-170056>
133. Janssens J, Hermans B, Vandermeeren M, Barale-Thomas E, Borgers M, Willems R, Meulders G, Wintmolders C, Van den Bulck D, Bittelbergs A, Ver Donck L, Larsen P, Moechars D, Edwards W, Mercken M, Van Broeck B (2021) Passive immunotherapy with a novel antibody against 3pE-modified A β demonstrates potential for enhanced efficacy and favorable safety in combination with BACE inhibitor treatment in plaque-depositing mice. *Neurobiol Dis* 154:105365. <https://doi.org/10.1016/j.nbd.2021.105365>
134. Wilcock DM, Colton CA (2009) Immunotherapy, vascular pathology, and microhemorrhages in transgenic mice. *CNS Neurol Disord Drug Targets* 8(1):50–64. <https://doi.org/10.2174/187152709787601858>
135. Taylor X, Clark IM, Fitzgerald GJ, Oluoch H, Hole JT, DeMattos RB, Wang Y, Pan F (2023) Amyloid-beta (A β) immunotherapy induced microhemorrhages are associated with activated perivascular macrophages and peripheral monocyte recruitment in Alzheimer's disease mice. *Mol Neurodegener* 18(1):59. <https://doi.org/10.1186/s13024-023-00649-w>
136. Wisniewski T, Goñi F (2015) Immunotherapeutic approaches for alzheimer's disease. *Neuron* 85(6):1162–1176. <https://doi.org/10.1016/j.neuron.2014.12.064>
137. Elmaleh DR, Farlow MR, Conti PS, Tompkins RG, Kundakovic L, Tanzi RE (2019) Developing effective alzheimer's disease therapies: clinical experience and future directions. *J Alzheimers Dis* 71(3):715–732. <https://doi.org/10.3233/JAD-190507>
138. Jucker M, Walker LC (2023) Alzheimer's disease: From immunotherapy to immunoprevention. *Cell* 186(20):4260–4270. <https://doi.org/10.1016/j.cell.2023.08.021>
139. Imbimbo BP, Balducci C, Ippati S, Watling M (2023) Initial failures of anti-tau antibodies in Alzheimer's disease are reminiscent of the amyloid-beta story. *Neural Regen Res* 18(1):117–118. <https://doi.org/10.4103/1673-5374.340409>
140. Vieira P, Rajewsky K (1986) The bulk of endogenously produced IgG2a is eliminated from the serum of adult C57BL/6 mice with a half-life of 6–8 days. *Eur J Immunol* 16(7):871–874. <https://doi.org/10.1002/eji.1830160727>
141. Vieira P, Rajewsky K (1988) The half-lives of serum immunoglobulins in adult mice. *Eur J Immunol* 18(2):313–316. <https://doi.org/10.1002/eji.1830180221>
142. Agadjanyan MG, Zagorski K, Petrushina I, Davtyan H, Kazarian K, Antonenko M, Davis J, Bon C, Blurton-Jones M, Cribbs DH, Ghochikyan A (2017) Humanized monoclonal antibody armanezumab specific to N-terminus of pathological tau: characterization and therapeutic potency. *Mol Neurodegener* 12(1):33. <https://doi.org/10.1186/s13024-017-0172-1>
143. Banks WA, Terrell B, Farr SA, Robinson SM, Nonaka N, Morley JE (2002) Passage of amyloid beta protein antibody across the blood-brain barrier in a mouse model of Alzheimer's disease. *Peptides* 23(12):2223–2226. [https://doi.org/10.1016/s0196-9781\(02\)00261-9](https://doi.org/10.1016/s0196-9781(02)00261-9)
144. Gallego-Rudolf J, Wiesman AI, Pichet Binette A, Villeneuve S, Baillet S, PREVENT-AD research group (2024) Synergistic association of A β and tau pathology with cortical neurophysiology and cognitive decline in asymptomatic older adults. *Nat Neurosci* 27(11):2130–2137. <https://doi.org/10.1038/s41593-024-01763-8>
145. Guo JP, Arai T, Miklossy J, McGeer PL (2006) A β and tau form soluble complexes that may promote self aggregation of both into the insoluble forms observed in Alzheimer's disease. *Proc Natl Acad Sci U S A* 103(6):1953–1958. <https://doi.org/10.1073/pnas.0509386103>
146. Miller Y, Ma B, Nussinov R (2011) Synergistic interactions between repeats in tau protein and A β amyloids may be responsible for accelerated aggregation via polymorphic states. *Biochemistry* 50(23):5172–5181. <https://doi.org/10.1021/bi200400u>
147. Vasconcelos B, Stancu IC, Buist A, Bird M, Wang P, Vanoosthuysen A, Van Kolen K, Verheyen A, Kienlen-Campard P, Octave JN, Baatsen P, Moechars D, Dewachter I (2016) Heterotypic seeding of Tau fibrillization by pre-aggregated A β provides potent seeds for prion-like seeding and propagation of Tau-pathology in vivo. *Acta Neuropathol* 131(4):549–569. <https://doi.org/10.1007/s00401-015-1525-x>
148. Ren B, Zhang Y, Zhang M, Liu Y, Zhang D, Gong X, Feng Z, Tang J, Chang Y, Zheng J (2019) Fundamentals of cross-seeding of amyloid proteins: an introduction. *J Mater Chem B* 7(46):7267–7282. <https://doi.org/10.1039/c9tb01871a>
149. Griner SL, Seidler P, Bowler J, Murray KA, Yang TP, Sahay S, Sawaya MR, Cascio D, Rodriguez JA, Philipp S, Sosna J, Glabe CG, Gonen T, Eisenberg DS (2019) Structure-based inhibitors of amyloid beta core suggest a common interface with tau. *Elife* 8:e46924. <https://doi.org/10.7554/eLife.46924>
150. Tripathi T, Khan H (2020) Direct interaction between the β -amyloid core and tau facilitates cross-seeding: a novel target for therapeutic intervention. *Biochemistry* 59(4):341–342. <https://doi.org/10.1021/acs.biochem.9b01087>
151. Giorgio J, Adams JN, Maass A, Jagust WJ, Breakspear M (2024) Amyloid induced hyperexcitability in default mode network drives medial temporal hyperactivity and early tau accumulation. *Neuron* 112(4):676–686. <https://doi.org/10.1016/j.neuron.2023.11.014>
152. Corsetti V, Florenzano F, Atlante A, Bobba A, Ciotti MT, Natale F, Della Valle F, Borreca A, Manca A, Meli G, Ferraina C, Feligioni M, D'Aguzzo S, Bussani R, Ammassari-Teule M, Nicolin V, Calissano P, Amadoro G (2015) NH2-truncated human tau induces deregulated mitophagy in neurons by aberrant recruitment of Parkin and UCHL-1: implications in Alzheimer's disease. *Hum Mol Genet* 24(11):3058–3081. <https://doi.org/10.1093/hmg/ddv059>
153. Di Natale G, Bellia F, Sciacca MFM, Campagna T, Pappalardo G (2018) Tau-peptide fragments and their copper(II) complexes: effects on amyloid- β aggregation. *Inorg Chim Acta* 472:82–92. <https://doi.org/10.1016/j.ica.2017.09.061>
154. Di Natale G, Sabatino G, Sciacca MFM, Tosto R, Milardi D, Pappalardo G (2022) A β and tau interact with metal ions, lipid membranes and peptide-based amyloid inhibitors: are these common features relevant

- in alzheimer's disease? *Molecules* 27(16):5066. <https://doi.org/10.3390/molecules27165066>
155. Bright J, Hussain S, Dang V, Wright S, Cooper B, Byun T, Ramos C, Singh A, Parry G, Stagliano N, Griswold-Prenner I (2015) Human secreted tau increases amyloid-beta production. *Neurobiol Aging* 36:693–709
156. Mukrasch MD, Bibow S, Korukottu J, Jeganathan S, Biernat J, Griesinger C, Mandelkow E, Zweckstetter M (2009) Structural polymorphism of 441-residue tau at single residue resolution. *PLoS Biol* 7(2):e34. <https://doi.org/10.1371/journal.pbio.1000034>
157. Perini G, Ciasca G, Minelli E, Papi M, Palmieri V, Maulucci G, Nardini M, Latina V, Corsetti V, Florenzano F, Calissano P, De Spirito M, Amadoro G (2019) Dynamic structural determinants underlie the neurotoxicity of the N-terminal tau 26–44 peptide in Alzheimer's disease and other human tauopathies. *Int J Biol Macromol* 141:278–289. <https://doi.org/10.1016/j.ijbiomac.2019.08.220>
158. Congdon EE, Ji C, Tetlow AM, Jiang Y, Sigurdsson EM (2023) Tau-targeting therapies for Alzheimer disease: current status and future directions. *Nat Rev Neurol* 19:715–736. <https://doi.org/10.1038/s41582-023-00883-2>
159. Hatami A, Albay R 3rd, Monjazeb S, Milton S, Glabe C (2014) Monoclonal antibodies against A β 42 fibrils distinguish multiple aggregation state polymorphisms in vitro and in Alzheimer disease brain. *J Biol Chem* 289:32131–32143. <https://doi.org/10.1074/jbc.M114.594846>

Publisher's Note

Springer Nature remains neutral with regard to jurisdictional claims in published maps and institutional affiliations.